

Order Determination for Spiked Models

Yicheng Zeng and Lixing Zhu*

Department of Mathematics, Hong Kong Baptist University, Hong Kong

Abstract

Motivated by dimension reduction in regression analysis and signal detection, we investigate the order determination for large dimension matrices including spiked models of which the numbers of covariates are proportional to the sample sizes for different models. Because the asymptotic behaviour of the estimated eigenvalues of the corresponding matrices differ completely from those in fixed dimension scenarios, we then discuss the largest possible number we can identify and introduce a “valley-cliff” criterion. We propose two versions of the criterion: one based on the original differences of eigenvalues and the other based on the transformed differences, which reduces the effects of ridge selection in the former one. This generic method is very easy to implement and computationally inexpensive, and it can be applied to various matrices. As examples, we focus on spiked population models, spiked Fisher matrices and factor models with auto-covariance matrices. Numerical studies are conducted to examine the method’s finite sample performances and to compare it with existing methods.

Keywords: Auto-covariance matrix, factor model, finite-rank perturbation, Fisher matrix, phase transition, ridge ratio, spiked population model.

*The authors gratefully acknowledge the support from a grant from the University Grants Council of Hong Kong, Hong Kong, and an SNFC grant (NSFC11671042) from the National Natural Science Foundation of China.

1 Introduction

Large dimensional matrices are often required to determine the order in diverse research fields to reduce the dimensionality. Examples include spiked population models proposed by [Johnstone \(2001\)](#); spiked Fisher matrices, which are motivated from signal detection and hypothesis testing for covariances; canonical correlation analysis; factor models; and target matrices in sufficient dimension reduction (see [Li \(1991\)](#); [Zhu et al. \(2010\)](#)), which are for sufficient dimension reduction in regression analysis, in particular. [Luo and Li \(2016\)](#) is a useful reference on order determination that proposed a ladle estimation for several models. We first use spiked population models as an example to describe the problem under study in this paper and propose a method that can be extended to handle other models. For any spiked population model, population covariance matrix Σ_p can be written as a finite-rank perturbation of the identity matrix: $\Sigma_p = \sigma^2 \mathbf{I}_p + \Delta_p$, where $\text{rank}(\Delta_p) = q$ amounts to the fixed number of spikes, and p is the dimension of the matrix. Thus, determining the number of spikes is equivalent to determining the order of the matrix Δ mentioned above. For other large dimensional matrices, such as sample auto-covariance matrices and spiked Fisher matrices, the problems can be formulated in a similar manner.

The literature includes several proposals in the fixed dimension cases, such as the classic Akaike Information Criteria and Bayesian Information Criteria. Several methods have been developed for sufficient dimension reduction that can also be used in the models mentioned above. The methods include the sequential testing method ([Li \(1991\)](#)), the BIC-type criterion ([Zhu et al. \(2006\)](#)), ridge ratio estimation ([Xia et al. \(2015\)](#)) and ladle estimation ([Luo and Li \(2016\)](#)). Some of them can even handle cases with divergent dimension problems in which $p/n \rightarrow 0$ at certain rates.

However, when the dimension p is proportional to the sample size n where $p/n \rightarrow c$ for $0 < c < \infty$, the problem becomes much more challenging. Thus, some efforts have been devoted to this problem with use of the large dimensional random matrix theory (see for example [Kritchman and Nadler \(2008\)](#); [Onatski \(2009\)](#)). Again, consider spiked

population models. When $p/n \rightarrow c$ for a constant $c > 0$, using the results derived by [Baik and Silverstein \(2006\)](#), [Passemier and Yao \(2012\)](#) introduced a criterion that counts the number of differences between two consecutive eigenvalues below a predetermined positive constant threshold. However, when there are equal spikes, the corresponding differences could also be smaller than the threshold they designed, and the criterion could then very easily define a smaller estimator than the true number. [Passemier and Yao \(2014\)](#) further modified this method to suit cases with multiple spikes. Underestimation however remains an issue when, say, there are three or more equal spikes. In addition to the problem caused by spike multiplicity, the dominating effect by a couple of the largest eigenvalues also results in underestimation. That is, when a couple of eigenvalues are very large and the other eigenvalues are too close to σ^2 and the differences between these small spikes would also be very small. For the number of factors from a factor model for high-dimensional time series, [Li et al. \(2017\)](#) proposed a similar criterion to that of [Passemier and Yao \(2014\)](#). For spiked Fisher matrices, [Wang and Yao \(2017\)](#) used the classical scree plot to determine the number of spikes when a threshold is selected in a delicate manner. The underestimation is still an issue. We demonstrate this phenomenon in the numerical studies below. Relevant references include [Lam and Yao \(2012\)](#) and [Xia et al. \(2015\)](#).

In this paper, we introduce a novel and generic criterion when the dimension p is proportional to the sample size n . The criterion is based on the eigenvalue difference-based ridge ratios with the following features. First, the criterion can handle spike multiplicity problem and alleviates the large eigenvalue dominance problem. Second, the criterion has a nice “valley-cliff” pattern such that the consistent estimator is at the “valley bottom” facing the “cliff” upon which all the next ratios exceed a threshold. Third, adding ridge values plays a very important role to make the ratios more stable and creates the “valley-cliff” pattern. Fourth, to reduce the sensitivity of the criterion to ridge selection, we suggest another version that uses transformed eigenvalues. Fifth, we also discuss in detail reducing the effect of model scale in the construction. The new method is also very efficient in computation.

The remainder of this paper is organised as follows. In Section 2, we propose a Valley-Cliff Estimation (VACLE) and provide an optimal lower bound to show what order can be identified. In Section 3, we first note that the VACLE could be improved when we use a transformation-based valley-cliff estimation (TVACLE) to alleviate the criterion's sensitivity to the designed ridge value. In this section, we also discuss in detail the methods to select transformation. In Section 4, we give spiked population models, factor models with auto-covariance matrices and spiked Fisher matrices as applications. Section 5 contains numerical studies and compares the VACLE and the TVACLE with existing competitors. A real data example is analysed in Section 6. Some concluding remarks are in Section 7, and the proofs of the theoretical results are contained in the supplementary materials.

2 Criterion construction and properties

In this section, we describe our motivation in detail and provide the construction steps and its properties.

2.1 Motivation

Consider a simple spiked population model. For a $p \times p$ matrix $\Sigma_p = \sigma^2 \mathbf{I}_p + \Delta_p$ with the eigenvalues $\lambda_1 \geq \dots \geq \lambda_{q_1} > \lambda_{q_1+1} = \dots = \lambda_p = \sigma^2$ where q_1 is a fixed number and the scale parameter σ^2 is either known or unknown. Let $\tilde{\lambda}_i$ be the eigenvalues of Δ_p and then $\lambda_i = \tilde{\lambda}_i + \sigma^2$, $1 \leq i \leq p$, with $\tilde{\lambda}_1 \geq \dots \geq \tilde{\lambda}_{q_1} > \tilde{\lambda}_{q_1+1} = \dots = \tilde{\lambda}_p = 0$. When p is proportional to n , estimation of $\lambda_i - \sigma^2$ is no longer consistent to 0. Thus, we do not directly use either λ_i or $\tilde{\lambda}_i$ but rather $\delta_i = \lambda_i - \lambda_{i+1} = \tilde{\lambda}_i - \tilde{\lambda}_{i+1} \geq 0$ for $i = 1, \dots, q_1$ and $= 0$ for $i = q_1 + 1, \dots, p - 1$. Consider a sequence of ratios as $r_i := \delta_{i+1}/\delta_i$, $1 \leq i \leq p - 2$. These ratios are scale-invariant and can then have the following property, when $i \leq q_1$:

$$r_i = \frac{\delta_{i+1}}{\delta_i} = \frac{\delta_{i+1}/\sigma^2}{\delta_i/\sigma^2} = \begin{cases} \geq 0, & \text{for } i < q_1, \\ = 0, & \text{for } i = q_1. \end{cases} \quad (2.1)$$

For any $q_1 + 1 \leq i \leq p - 2$, $r_i = 0/0$ cannot be well defined because the values could vary dramatically and thus be instable. Due to the non-monotonicity of the δ_i 's, some ratios r_i , even for $1 \leq i \leq q_1$, could converge to either $*/0$, $0/*$, $0/0$ or $*/*$ respectively, where $*$ stands for a positive value that could differ for each appearance. This instability also occurs at the sample level. Thus, we cannot simply use this sequence of ratios to construct a criterion. Taking these into consideration, we define a sequence of ridge type ratios:

$$r_i^R := \frac{\delta_{i+1}/\sigma^2 + c_n}{\delta_i/\sigma^2 + c_n}, 1 \leq i \leq p - 2. \quad (2.2)$$

It is noticeable, in the construction of r_i^R , that we use δ_i/σ^2 instead of δ_i in order to keep selection of c_n independent of the scale parameter σ^2 . With appropriately selected $c_n \rightarrow 0$, these ratios have the following property:

$$r_i^R = \frac{\delta_{i+1}/\sigma^2 + c_n}{\delta_i/\sigma^2 + c_n} = \begin{cases} \geq 0, & \text{for } i < q_1, \\ = c_n/(\delta_{q_1}/\sigma^2 + c_n) \rightarrow 0, & \text{for } i = q_1, \\ c_n/c_n = 1, & \text{for } q_1 + 1 \leq i \leq p - 2, \end{cases}$$

These ratios have a very useful “valley-cliff” pattern, because q_1 should be the index of $r_{q_1}^R \rightarrow 0$ at a “valley bottom” facing the “cliff” valued at 1 of all next ratios r_i^R for $i > q_1$. This nice pattern gives us a good opportunity to accurately identify q_1 , although we will show later that in the setting in which p is proportional to the sample size n , the identifiability of q_1 at the sample level remains a serious issue.

We also note that the ratios depend on σ^2 and c_n . Under the aforementioned scale transformation $\hat{\lambda}_i \mapsto (\sigma^2)^{-1}\hat{\lambda}_i$, if $\hat{\lambda}_i$ are the estimated eigenvalues,

$$\hat{r}_i^R = \frac{\hat{\delta}_{i+1}/\sigma^2 + c_n}{\hat{\delta}_i/\sigma^2 + c_n} = \frac{(\sigma^2)^{-1}\hat{\lambda}_{i+1} - (\sigma^2)^{-1}\hat{\lambda}_{i+2} + c_n}{(\sigma^2)^{-1}\hat{\lambda}_i - (\sigma^2)^{-1}\hat{\lambda}_{i+1} + c_n} = \frac{\hat{\lambda}_{i+1} - \hat{\lambda}_{i+2} + \sigma^2 c_n}{\hat{\lambda}_i - \hat{\lambda}_{i+1} + \sigma^2 c_n}.$$

Later, however, we will show that the range of selecting c_n can be rather wide, and thus the criterion is not very seriously affected by this cost when σ^2 is estimated, which can be shown in the numerical studies we conduct later. In addition, we have a brief discussion about the estimation of σ^2 in Section 5.

2.2 Valley-cliff criterion and estimation consistency

Let \mathbf{T}_n be a target sample matrix of Σ_p and $\hat{\lambda}_1 \geq \dots \geq \hat{\lambda}_p$ be its eigenvalues. Here notations $\hat{\lambda}_i$ and $\hat{\delta}_i$ are related to the sample size n , although the n 's in subscripts have been omitted for brevity. Define their sample versions \hat{r}_i^R of r_i^R in (2.2) with $\hat{\delta}_i = \hat{\lambda}_i - \hat{\lambda}_{i+1}$ as

$$\hat{r}_i^R := \frac{\hat{\delta}_{i+1}/\sigma^2 + c_n}{\hat{\delta}_i/\sigma^2 + c_n}, \quad 1 \leq i \leq p-2, \quad (2.3)$$

where σ^2 should be replaced by $\hat{\sigma}^2$ when σ^2 is unknown.

However, completely unlike the case with fixed p , even in the simple spiked population model case, $\hat{\lambda}_i$ are not consistent to λ_i and these ratios cannot then simply converge to those in (2.1). The number q_1 is generally unidentifiable. In the following section, we give the largest possible order we can identify. Define

$$q := \#\{i : 1 \leq i \leq q_1, \lambda_i > U(F) > \sigma^2\} \quad (2.4)$$

for some constant $U(F)$ where F is the limiting spectral distribution (LSD) of all estimated eigenvalues $\hat{\lambda}_i$'s with the support $(a(F), b(F))$. The constant $U(F)$ is the phase transition point (see Baik and Silverstein (2006)) and also the optimal bound for identifiability. We still use a spiked population model as a typical example. From Baik et al. (2005) and Baik and Silverstein (2006), any spike with strength not stronger than $(1 + \sqrt{c})\sigma^2$ is not identifiable. In this case, $U(F)$ refers to the critical value $(1 + \sqrt{c})\sigma^2$. More details are included in Section 4.

Selecting an appropriate sequence c_n plays an important role for estimation efficiency. When it is selected in the principle: $\hat{\delta}_i = o_p(c_n)$ for $q+1 \leq i \leq p-1$, \hat{r}_i^R still have a nice ‘‘valley-cliff’’ pattern at $i = q$ as

$$\lim_{n \rightarrow +\infty} \hat{r}_i^R = \begin{cases} 0, & i = q \\ 1, & q+1 \leq i \leq L-1 \end{cases} \quad (2.5)$$

where L is a prefixed upper bound for q . Taking this advantage, we define a thresholding valley-cliff estimator as, for a constant τ with $0 < \tau < 1$

$$\hat{q}_n^{VACLE} = \max_{1 \leq i \leq L-2} \{i : \hat{r}_i^R \leq \tau\}. \quad (2.6)$$

To handle more general models, we consider the large dimensional matrices with the following model features.

Model Feature 2.1. *There exists a bound $U(F)$ such that the number q defined in (2.4) is a fixed constant and satisfies:*

(A1) *there is a value d such that $\hat{\lambda}_q/\sigma^2 - d = o_P(1)$ as $n \rightarrow \infty$;*

(A2) *for a large fixed value L satisfying $q + 1 < L < p$, there is a constant $e < d$ and a sequence $\tilde{c}_n \rightarrow 0$ such that $\hat{\lambda}_i/\sigma^2 - e = O_p(\tilde{c}_n)$, for $q + 1 \leq i \leq L$.*

Remark 2.1. *Model Feature 2.1 describes features of the model structure at the sample level, that essentially requires certain assumptions at the population level. Condition (A1) corresponds to the so-called phase transition phenomenon for the extreme eigenvalues, and (A2) further focuses on the fluctuations of those that stick to the boundary of the support of the LSD. General theory about the phase transitions and fluctuations can be found, for example, in [Péché \(2006\)](#), [Benaych-Georges et al. \(2011\)](#), [Benaych-Georges and Nadakuditi \(2011\)](#) and [Knowles and Yin \(2017\)](#). The details about how these features can be exhibited in three types of models are given in Section 4.*

The estimation consistency is stated as follows.

Theorem 2.1. *When a model satisfies Model Feature 2.1, and $\tilde{c}_n = o(c_n)$, then $\mathbb{P}(\hat{q}_n^{VACLE} = q) \rightarrow 1$ as $n \rightarrow \infty$.*

Remark 2.2. *The convergence rate of $\hat{\lambda}_i$ to a constant e , for $q + 1 \leq i \leq L - 1$ is often $O_p(n^{-2/3})$, namely $\tilde{c}_n = n^{-2/3}$. The references include [Benaych-Georges et al. \(2011\)](#), [Bao et al. \(2015\)](#), [Han et al. \(2016\)](#) and [Han et al. \(2018\)](#) for several models discussed in Section 4. However, for a spiked auto-covariance matrix, we will also state our result provided, as [Li et al. \(2017\)](#) did, that this rate can be achieved as this rate has not yet formally been derived. In this paper, the ridge $c_n \rightarrow 0$ is only restricted to $\hat{\lambda}_{q+1} = o_p(c_n)$. Such a wide range for the ridge selection alleviates, to a great extent, the influence from σ^2 when it needs to be estimated. The estimation issue will be discussed in Section 5.*

3 Modification of the VACLE

Although Theorem 2.1 provides estimation consistency, some numerical studies that are not presented in this paper indicate that the performance of \hat{q}_n^{VACLE} is sometimes and somehow sensitive to the choice of the ridge c_n in finite sample cases. To be specific, when $d - e$ in Model Feature 2.1 is small, the ratio at q could be close to 1, and then we would easily determine a smaller value. Therefore, a small ridge c_n is in demand. On the other hand, a small c_n would result in the instability caused by 0/0 type ratios, and overestimation would be possible. Thus, a trade-off exists between underestimation and overestimation in the choice of ridge c_n . We now attempt to alleviate this dilemma by using transformed eigenvalues.

Considering a transformation (depending on n) $f_n(\cdot)$, define

$$\hat{\delta}_i^* = f_n(\hat{\lambda}_i/\sigma^2) - f_n(\hat{\lambda}_{i+1}/\sigma^2), \quad i = 1, 2, \dots, p-1. \quad (3.1)$$

The ratios are defined as

$$\hat{r}_i^{TR} := \frac{\hat{\delta}_{i+1}^* + c_n}{\hat{\delta}_i^* + c_n}, \quad 1 \leq i \leq p-2. \quad (3.2)$$

The estimator of q is defined as

$$\hat{q}_n^{TVACLE} = \max_{1 \leq i \leq L-2} \{i : \hat{r}_i^{TR} \leq \tau\}, \quad (3.3)$$

where c_n and τ have the same definitions as before. We call this criterion the transformation-based valley-cliff estimation(TVACLE).

For any transformation f_n , we wish that \hat{r}_i^{TR} remains close to 1 for $i > q$, and \hat{r}_q^{TR} is closer to zero than \hat{r}_q^R . To achieve these objectives, we consider a transformation that can satisfy the following requirements (i) – (iii):

- (i) $\mathbb{P}\{\hat{\delta}_q^* \geq \hat{\delta}_q/\sigma^2\} \rightarrow 1$;
- (ii) $\mathbb{P}\{\hat{\delta}_i^* \leq \hat{\delta}_i/\sigma^2\} \rightarrow 1$, for $q+1 \leq i \leq p-2$;
- (iii) $\hat{\delta}_{q+1}^*/\hat{\delta}_q^* \leq \hat{\delta}_{q+1}/\hat{\delta}_q$.

Remark 3.1. Conditions (i) and (ii) ensure the transformation could pull up the value of $\hat{\delta}_q$ and bring down that of $\hat{\delta}_i$, for $q + 1 \leq i \leq p - 2$. Condition (iii) is critical to ensuring that the “valley” could be closer to its limit “0” and then be better separated from the “cliff” after the transformation.

The following conditions (a) – (c) ensure that $f_n : \mathbb{R} \rightarrow \mathbb{R}$ satisfies the above requirements (i) – (iii), letting $f'_n(x)$ be the derivative of $f_n(x)$ with respect to x :

- (a) f_n is differentiable, and $f'_n \geq 0$ in \mathbb{R} ;
- (b) f'_n is increasing and nonnegative in \mathbb{R} ;
- (c) there exists a sequence $\kappa_n > 0$, $\hat{\lambda}_i/\sigma^2 - e = o_p(\kappa_n)$ for $q + 1 \leq i \leq L - 1$ such that $f'_n(x) = 1$ for all $x \in (e - \kappa_n, e + \kappa_n)$.

Lemma 3.1. Conditions (a)–(c) imply Requirements (i)–(iii) for $\{\hat{\delta}_{n,i}^*\}$ and $\{\hat{\delta}_{n,i}\}$ defined as above.

Remark 3.2. In Condition (c), κ_n can take a wide range of values, as long as it satisfies the condition that $\hat{\lambda}_i/\sigma^2 - e = o_p(\kappa_n)$ for $q + 1 \leq i \leq L - 1$. Specifically, it can take a constant value, converge to zero or even converge to infinity. Let f'_n take value 1 in a neighbourhood of the value e with radius κ_n , so that all $\hat{\lambda}_i/\sigma^2$, for $q + 1 \leq i \leq L - 1$, fall into this neighbourhood. Thus, the ratios \hat{r}_i^{TR} , for $q + 1 \leq i \leq L - 2$, remain unaffected by the transformation f_n . Besides, the selection of κ_n is independent of c_n .

We now give a piecewise quadratic function for this purpose as follows:

$$f_n(x) = \begin{cases} L_n - \frac{1}{2k_1}, & x < L_n - \frac{1}{k_1} \\ \frac{1}{2}k_1x^2 + (1 - k_1L_n)x + \frac{1}{2}k_1L_n^2, & L_n - \frac{1}{k_1} \leq x < L_n \\ x, & L_n \leq x < R_n \\ \frac{1}{2}k_2x^2 + (1 - k_2R_n)x + \frac{1}{2}k_2R_n^2, & x \geq R_n \end{cases} \quad (3.4)$$

where k_1 and k_2 are slopes of $\{f'_n\}_{n \geq 1}$ to be determined, $L_n = e - \kappa_n$, $R_n = e + \kappa_n$. It is clear that when k_1 and k_2 are 0, the TVACLE degenerates to the VACLE.

The consistency of \hat{q}_n^{TVACLE} is stated in the following theorem.

Theorem 3.1. *Under the same conditions of Theorem 2.1, the estimator \hat{q}_n^{TVACLE} with the above transformation f_n is equal to q with a probability going to 1.*

Remark 3.3. *Although selecting an optimal transformation is desirable, we suspect the existence as there are a large class of functions that could satisfy the conditions. Thus, such an issue is beyond the scope of this paper.*

4 Applications to several models

In this section, we introduce several special models to which our method can be applied.

Spiked population models The model can also be motivated from the signal detection problem (see, e.g. Nadler (2010)):

$$x_i = \mathbf{A}u_i + \varepsilon_i, \quad 1 \leq i \leq n, \quad (4.1)$$

where $u_i \in \mathbb{R}^q$ is a q -dimensional random signal vector with zero mean components, $\varepsilon_i \in \mathbb{R}^p$ is a p -dimensional random vector with mean zero and covariance matrix $\sigma^2 \mathbf{I}_p$, $\mathbf{A} \in \mathbb{R}^{p \times q}$ is the steering matrix whose q columns are linearly independent of each other and $x_i \in \mathbb{R}^p$ is the observed vector on the p sensors. Assume that the covariance matrix of the signals is of full rank with q largest eigenvalues $\lambda_1 \geq \dots \geq \lambda_q > \sigma^2 > 0$. With the typical high dimensional setting in which $p/n \rightarrow c \in (0, +\infty)$, the population covariance matrix Σ_p of x_i coincides with the structure of a spiked population model:

$$\text{spec}(\Sigma_p) = \{\lambda_1, \dots, \lambda_q, \sigma^2, \dots, \sigma^2\}, \quad (4.2)$$

Theoretically, the spiked population model allows the existence of small spikes (i.e. $\lambda_i < \sigma^2$), but this case is not discussed in this paper.

Theorem 4.1. *Suppose that $\lambda_q > U(F) = \sigma^2(1 + \sqrt{c})$. This bound is optimal for the identifiability of q . Model Feature 2.1 then holds, and the results of Theorems 2.1 and 3.1 hold true.*

Remark 4.1. *From the proof in the supplementary materials, we see the optimality of the lower bound $U(F) = \sigma^2(1 + \sqrt{c})$ because it is not possible to identify any eigenvalue λ_i such that $\sigma^2(1 + \sqrt{c}) > \lambda_i > \sigma^2$ for any $q < i \leq L$.*

Large-dimensional spiked Fisher matrix Again consider the signal detection problem discussed above,

$$x_i = \mathbf{A}u_i + \varepsilon_i, \quad 1 \leq i \leq n, \quad (4.3)$$

where x_i , \mathbf{A} and u_i share the same settings of (4.1), whilst ε_i is a noise vector with a general covariance matrix Σ_2 . Denote the population covariance matrix of x_i by Σ_1 such that $\Sigma_1 = \Sigma_2 + \Delta$, where $\Delta = \mathbf{A}cov(u_i)\mathbf{A}^T$ is a non-negative definite matrix with fixed rank q provided that $cov(u_i)$ is of full rank. If $\Sigma_1 = \sigma^2\mathbf{I}_p$, it degenerates to the spiked population model. Otherwise, we note that $\Sigma_1\Sigma_2^{-1}$ has a spiked structure as

$$\text{spec}(\Sigma_1\Sigma_2^{-1}) = \{\lambda_1, \dots, \lambda_q, 1, \dots, 1\}, \quad (4.4)$$

where $\lambda_1 \geq \dots \geq \lambda_q > 1$ and the number of spikes q is fixed. Let \mathbf{S}_1 and \mathbf{S}_2 be the sample covariance matrices that correspond to Σ_1 and Σ_2 with respective sample sizes of n and T , where $p/n \rightarrow c > 0$ and $p/T \rightarrow y \in (0, 1)$ as $n \rightarrow \infty$ and $T \rightarrow \infty$ respectively. Note that there are two different sample sizes n and T because the sample covariance matrix \mathbf{S}_2 comes from another sequence of pure noise observations, say $\{e_i\}_{1 \leq i \leq T}$, with a different sample size T . Denote $\mathbf{S}_1 = \frac{1}{n} \sum_{i=1}^n x_i x_i^\top$ and $\mathbf{S}_2 = \frac{1}{T} \sum_{i=1}^n e_i e_i^\top$. When \mathbf{S}_2 is invertible, the random matrix $\mathbf{F}_n = \mathbf{S}_1 \mathbf{S}_2^{-1}$ is called a Fisher matrix, whose motivation comes from the following hypothesis testing problem:

$$H_0 : \Sigma_1 = \Sigma_2 \quad H_1 : \Sigma_1 = \Sigma_2 + \Delta. \quad (4.5)$$

See Wang and Yao (2017) as an example. Denote the eigenvalues of \mathbf{F}_n as $\hat{\lambda}_1 \geq \dots \geq \hat{\lambda}_p$. The difference between the two hypotheses then relies upon those extreme eigenvalues of \mathbf{F}_n .

We consider a more general Fisher matrix with the spiked structure

$$\text{spec}(\Sigma_1 \Sigma_2^{-1}) = \{\lambda_1, \dots, \lambda_q, \sigma^2, \dots, \sigma^2\}. \quad (4.6)$$

This is motivated by the hypothesis testing problem:

$$H_0 : \Sigma_1 = \sigma^2 \Sigma_2 \quad H_1 : \Sigma_1 = \sigma^2 \Sigma_2 + \Delta, \quad (4.7)$$

Also, by using the simple transformation $\hat{\lambda}_i \mapsto (\sigma^2)^{-1} \hat{\lambda}_i$, we can achieve the results in the case of $\sigma^2 = 1$ in a similar manner.

Theorem 4.2. *Suppose that $\lambda_q > U(F) = \sigma^2 \gamma (1 + \sqrt{c + y - cy})$, where $\gamma = (1 - y)^{-1}$. This is the optimal lower bound for identifiability of q , and Model Feature 2.1 holds. The results of Theorems 2.1 and 3.1 hold true.*

In the following section, we consider the auto-covariance matrix. This matrix has a more much complicated structure at the sample level, so we provide some more discussion that does not exactly follow the examination for the Model Feature 2.1 in Theorems 2.1 and 3.1. In addition, because the theoretical analysis for the estimated matrix is not as complete as those for the spiked population and Fisher matrix, we must then add some extra assumptions on the convergence rate of the estimated eigenvalues if we wish to derive the estimation consistency, although it would be true, as reasonably conjectured by Li et al. (2017). This requires a rigorous proof, but it is beyond the scope of this paper. We shall therefore leave it to a further study. In this paper, however, we provide a proposition that assumes that the convergence rate can be achieved and use numerical studies to verify the usefulness of our method in practice.

Large dimensional auto-covariance matrix Consider a factor model:

$$y_t = \mathbf{A}x_t + \varepsilon_t, \quad (4.8)$$

where for a fixed number q_0 , x_t is a q_0 -dimensional common factor time series, \mathbf{A} is the $p \times q_0$ factor loading matrix, $\{\varepsilon_t\}$ is a sequence of Gaussian noise independent of x_t and

y_t is the t -th column of the $p \times T$ observed matrix \mathbf{Y} ; namely, p -dimensional observation at time t . Let $\Sigma_y = \text{cov}(y_t, y_{t-1})$ be the lag-1 auto-covariance matrices of y_t , and let $\hat{\Sigma}_y = \frac{1}{T} \sum_{t=2}^{T+1} y_t y_{t-1}^\top$ be its sample version.

Let μ be a finite measure on the real line \mathbb{R} with support denoted by $\text{supp}(\mu)$ and $\mathbb{C} \setminus \text{supp}(\mu)$ be a complex space \mathbb{C} subtracting the set $\text{supp}(\mu)$. For any $z \in \mathbb{C} \setminus \text{supp}(\mu)$, the Stieltjes transformation and T-transformation of μ are respectively defined as

$$\mathcal{S}(z) = \int \frac{1}{t-z} d\mu(t), \quad \mathcal{T}(z) = \int \frac{t}{z-t} d\mu(t). \quad (4.9)$$

When μ is supported on an interval, say $\text{supp}(\mu) = [A, B]$, and z is a real value, the T-transformation $\mathcal{T}(\cdot)$ is a decreasing homeomorphism from $(-\infty, A)$ onto $(\mathcal{T}(A-), 0)$ and from $(B, +\infty)$ onto $(0, \mathcal{T}(B+))$, where

$$\mathcal{T}(A-) := \lim_{z \in \mathbb{R}, z \rightarrow A-} \mathcal{T}(z), \quad \mathcal{T}(B+) := \lim_{z \in \mathbb{R}, z \rightarrow B+} \mathcal{T}(z).$$

Give the assumptions on the time series $\{x_t\}_{1 \leq t \leq T}$ and $\{\varepsilon_t\}_{1 \leq t \leq T}$ (Li et al. (2017)) as follows.

Assumption 4.1. $\{x_t\}_{1 \leq t \leq T}$ is a q_0 -dimensional stationary time series, where q_0 is a fixed number. Every component is independent of the others,

$$x_{i,t} = \sum_{l=0}^{\infty} \alpha_{i,l} \eta_{i,t-l}, \quad i = 1, \dots, q_0, \quad t = 1, \dots, T,$$

where $\{\eta_{i,k}\}$ is a real-valued and weakly stationary white noise with mean 0 and variance σ_i^2 . Denote $\gamma_0(i)$ and $\gamma_1(i)$ as the variance and lag-1 auto-covariance of $\{x_{i,t}\}$, respectively.

Assumption 4.2. $\{\varepsilon_t\}$ is a p -dimensional real-valued random vector independent of $\{x_t\}$ and with independent components $\varepsilon_{i,t}$, satisfying $\mathbb{E}(\varepsilon_{i,t}) = 0$, $\mathbb{E}(\varepsilon_{i,t}^2) = \sigma^2$, and $\forall \eta > 0$,

$$\frac{1}{\eta^4 p^T} \sum_{i=1}^p \sum_{t=1}^{T+1} \mathbb{E}(|\varepsilon_{i,t}|^4 I_{(|\varepsilon_{i,t}| \geq \eta T^{1/4})}) \longrightarrow 0 \quad \text{as } pT \rightarrow \infty.$$

In the high dimensional setting with $p/T \rightarrow y > 0$, the following result holds.

Proposition 4.1. Denote $\mathcal{T}(\cdot)$ as the T -transformation of the limiting spectral distribution for matrix $\hat{\mathbf{M}}_y/\sigma^4 \equiv \hat{\Sigma}_y \hat{\Sigma}_y^\top/\sigma^4$. Suppose that the above assumptions are satisfied. Let $q = \#\{i : 1 \leq i \leq q_0, \mathcal{T}_1(i) < \mathcal{T}(b_1+)\}$, where

$$\mathcal{T}_1(i) = \frac{2y\sigma^2\gamma_0(i) + \gamma_1(i)^2 - \sqrt{(2y\sigma^2\gamma_0(i) + \gamma_1(i)^2)^2 - 4y^2\sigma^4(\gamma_0(i)^2 - \gamma_1(i))^2}}{2\gamma_0(i)^2 - 2\gamma_1(i)^2},$$

$$b_1 = (-1 + 20y + 8y^2 + (1 + 8y)^{3/2})/8, \quad \mathcal{T}(b_1+) = \lim_{z \in \mathbb{R}, z \rightarrow b_1+} \mathcal{T}(z).$$

Then q is the largest number of common factors that are identifiable.

Remark 4.2. Although the constraint $\mathcal{T}_1(i) < \mathcal{T}(b_1+)$ does not have a simple formulation presented in Model Feature 2.1, it also provides the optimal bound.

Proposition 4.2. If the estimated eigenvalues $\hat{\lambda}_i$ for $i > q$ have a convergence rate of order $O_p(n^{-2/3})$ with the assumptions in Proposition 4.1, Model Feature 2.1 then holds, and Theorems 2.1 and 3.1 hold true.

Remark 4.3. As we commented before, [Li et al. \(2017\)](#) considered a criterion with a reasonable conjecture on the convergence rate of order $O_p(n^{-2/3})$, although without a rigorous proof. We have not provided this result either, and thus we regard the above result as a proposition, rather than a theorem. We will see that it works well in the numerical studies.

5 Numerical Studies

5.1 Scale estimation

[Passemier and Yao \(2012\)](#) estimated σ^2 by simply taking the average over $\{\hat{\lambda}_i\}_{q+1 \leq i \leq p}$ and [Passemier et al. \(2017\)](#) established its consistency and further introduced a refined version by subtracting the bias. That, however, involves an iteration procedure because the number q must be estimated. To construct a robust estimator, [Ulfarsson and Solo \(2008\)](#) and [Johnstone and Lu \(2009\)](#) used the median of the sample eigenvalues $\{\hat{\lambda}_i : \hat{\lambda}_i \leq b\}$ and the sample variances $\{\frac{1}{n} \sum_{i=1}^n x_{ij}^2\}_{1 \leq j \leq p}$, respectively. The former median still requires a

crude estimator of the right edge $b = \sigma^2(1 + \sqrt{c})^2$ in advance, which is equivalent to give a rough initial estimator of σ^2 .

In this section, we propose a one-step procedure that could be regarded as a simplified version of the method of [Ulfarsson and Solo \(2008\)](#). With spiked population models, the empirical spectral distribution of \mathbf{S}_n almost surely converges to a Marcenko-Pastur distribution $F_{c,\sigma^2}(x)$ (see details in Supplementary Materials). For $0 < \alpha < 1$, their α -quantiles are denoted $\hat{\xi}_{c,\sigma^2}^{(n)}(\alpha)$ and $\xi_{c,\sigma^2}(\alpha)$, respectively:

$$\hat{\xi}_{c,\sigma^2}^{(n)}(\alpha) := \hat{\lambda}_{p-[p\alpha]}, \quad \xi_{c,\sigma^2}(\alpha) := \inf\{x : F_{c,\sigma^2}(x) \geq \alpha\}. \quad (5.1)$$

It then follows that $\hat{\xi}_{c,\sigma^2}^{(n)}(\alpha) \rightarrow \xi_{c,\sigma^2}(\alpha)$, as $n \rightarrow \infty$. Note that $\xi_{c,\sigma^2}(\alpha) = \sigma^2 \xi_{c,1}(\alpha)$. Approximating a certain quantile, say $\xi_{c,\sigma^2}(\alpha)$, of the M-P distribution by its sample counterpart $\hat{\xi}_{c,\sigma^2}^{(n)}(\alpha)$, we obtain an estimator of σ^2 ,

$$\hat{\sigma}^2 = \hat{\xi}_{c,\sigma^2}^{(n)}(\alpha) \cdot \xi_{c,1}(\alpha)^{-1}. \quad (5.2)$$

The consistency of $\hat{\sigma}^2$ is equivalent to that of $\hat{\xi}_{c,\sigma^2}^{(n)}(\alpha)$, which can hold under certain conditions. Further, the rigidity of the eigenvalues of covariance matrix (see Theorem 3.3 in [Pillai and Yin \(2014\)](#)) implies that the convergence rate of $\hat{\sigma}^2$ is $o(n^{-1+\varepsilon})$ for any $\varepsilon > 0$. Thus, consistencies still hold for VACLE and TVACLE when we replace $\hat{\lambda}_i/\sigma^2$ by $\hat{\lambda}_i/\hat{\sigma}^2$, as $\hat{\sigma}^2$ possesses a higher convergence rate than those extreme eigenvalues $\hat{\lambda}_i$, $1 \leq i \leq L$ for any fixed L . Practically, for the sake of simplicity and stability, we let $\alpha = 0.5$ for $0 < c < 1$; and $1 - (2c)^{-1}$ for $c \geq 1$. Then $\alpha = 1 - (2 \max\{1, c\})^{-1}$. The sample quantile $\hat{\xi}_{c,\sigma^2}^{(n)}(\alpha)$ divides all positive eigenvalues of \mathbf{S}_n into two equal parts. The estimator $\hat{\sigma}^2$ is then less sensitive to extreme eigenvalues of \mathbf{S}_n . Its performance is examined in the following numerical studies.

5.2 Simulations about spiked population models

In this subsection, we consider the comparisons between VACLE and TVACLE defined as \hat{q}_n^{VACLE} and \hat{q}_n^{TVACLE} and the method defined as \hat{q}_n^{PY} developed and refined by [Passemier](#)

and Yao (2012) and Passemier and Yao (2014). Because estimating the number of spikes q is the main focus, we conduct the simulations mainly with given σ^2 . For unknown σ^2 , we give a brief discussion, and a simple one-step estimator of σ^2 is introduced in Section 5.1. In all simulation experiments, we conduct 500 independent replications. Furthermore, recalling the definition of $c = p/n$, we report the results with three scenarios: $c = .25, 1$ and 2 to represent the cases with dimensions p smaller than and larger than the sample size n , respectively. \hat{q}_n^{PY} is defined by

$$\hat{q}_n^{PY} = \min\{i \in \{1, \dots, Q\} : \hat{\delta}_{i+1} < d_n \text{ and } \hat{\delta}_{i+2} < d_n\}, \quad (5.3)$$

where $L > q$ is a prefixed bound large enough, $d_n = o(n^{-1/2})$ and $n^{2/3}d_n \rightarrow +\infty$.

Models and parameters selections: the known σ^2 case.

For \hat{q}_n^{PY} , the sequence $d_n = Cn^{-2/3}\sqrt{2\log\log n}$ with C being adjusted by an automatic procedure identical to that in Passemier and Yao (2014). For \hat{q}_n^{VACLE} and \hat{q}_n^{TVACLE} , they share the same threshold $\tau = 0.5$ but have different ridges c_n . Theoretically speaking, the selection range of c_n is very wide to meet the requirement that $c_n \rightarrow 0$ and $n^{2/3}c_n \rightarrow +\infty$. Here, we give an automatic procedure for ridge calibration by pure-noise simulations. For given (p, n) , we conduct 500 independent pure-noise simulations and obtain the α -quantile $q_{p,n}(\alpha)$ and sample mean $m_{p,n}$ of the difference $\{\hat{\lambda}_1 - \hat{\lambda}_2\}$, where $\hat{\lambda}_1$ and $\hat{\lambda}_2$ are the two largest eigenvalues of the noise matrix. By results in Benaych-Georges et al. (2011), for such a no-spike matrix, we can use $\{\hat{\lambda}_1 - \hat{\lambda}_2\}$ to approximate $\hat{\delta}_{q+1}$:

$$\begin{aligned} & \mathbb{P}\{q_{p,n}(0.01) - m_{p,n} < \hat{\delta}_{q+1} - m_{p,n} < q_{p,n}(0.99) - m_{p,n}\} \\ & \approx \mathbb{P}\{q_{p,n}(0.01) - m_{p,n} < \hat{\lambda}_1 - \hat{\lambda}_2 - m_{p,n} < q_{p,n}(0.99) - m_{p,n}\} \approx 0.98. \end{aligned}$$

Thus, the ratio $\left[\hat{\delta}_{q+2} - m_{p,n} + [q_{p,n}(0.99) - q_{p,n}(0.01)] \right] \left[\hat{\delta}_{q+1} - m_{p,n} + [q_{p,n}(0.99) - q_{p,n}(0.01)] \right]^{-1}$ would be dominated by the term $[q_{p,n}(0.99) - q_{p,n}(0.01) - m_{p,n}]$ and then remain close to the ‘‘cliff’’ valued at 1 with a high probability. To ensure the convergence rate, we select ridge $c_n^{(1)} = \log\log n \cdot [q_{p,n}(0.95) - q_{p,n}(0.05)] - m_{p,n}$ for the VACLE and a smaller one

$c_n^{(2)} = \sqrt{\log \log n} [q_{p,n}(0.95) - q_{p,n}(0.05)] - m_{p,n}$ for the TVACLE. Note that $q_{p,n}(\alpha)$ and $m_{p,n}$ converge to zero at the same rate as $\hat{\lambda}_{q+1}$ that has a slightly faster rate to zero than $c_n^{(1)}$ and $c_n^{(2)}$. In addition, we manually determine the sequence κ_n . Details in the parameters selections are reported in Table 1. Following the calibration procedure of [Passemier and Yao \(2014\)](#), we obtain the value of C for various $c = p/n$, as shown in Table 2.

Table 1: Parameters settings for the three methods.

Method	d_n	τ	c_n	κ_n	k_1	k_2	L
PY	$C \cdot n^{-2/3} \sqrt{2 \log \log n}$	—	—	—	—	—	20
VACLE	—	0.5	$c_n^{(1)}$	—	—	—	20
TVACLE	—	0.5	$c_n^{(2)}$	$\log \log p \cdot p^{-2/3}$	5	5	20

Table 2: Values of C .

$c=p/n$	0.25	1	2
C	5.5226	6.3424	7.6257

Remark 5.1. *Note that we select different ridges c_n in \hat{q}_n^{VACLE} and \hat{q}_n^{TVACLE} . As described above, a relatively small ridge c_n could cause \hat{r}_{q+1}^R to have better separation from \hat{r}_q^R , but it might also result in instability of \hat{r}_i^R for $i > q + 1$, so a relatively large ridge is needed for \hat{r}_i^R . However, \hat{r}_i^{TR} would be much less sensitive to the ridge. Thus, we choose a smaller ridge for \hat{q}_n^{TVACLE} . Besides, ridges $c_n^{(1)}$ and $c_n^{(2)}$ are generated by an automatic procedure instead of manual selections. This calibration procedure only depends on (p, n) .*

Consider three models: for fair comparison, Models 1 and 2 were used by [Passemier and Yao \(2012\)](#) with dispersed spikes and closely spaced but unequal spikes respectively, and Model 3 has two equal spikes:

Model 1. $q = 5$, $(\lambda_1, \dots, \lambda_5) = (259.72, 17.97, 11.04, 7.88, 4.82)$,

Model 2. $q = 4$, $(\lambda_1, \dots, \lambda_4) = (7, 6, 5, 4)$,

Model 3. $q = 4$, $(\lambda_1, \dots, \lambda_4) = (5, 4, 3, 3)$.

Furthermore, we compare \hat{q}_n^{TVACLE} with \hat{q}_n^{PY} on a model with greater multiplicity of spikes:

Model 4. $q = 6$, $(\lambda_1, \dots, \lambda_6) = (5, 5, 5, 5, 5, 5)$.

Set $\sigma^2 = 1$. When σ^2 is regarded as unknown, use the one-step method in (5.2) to estimate it. We conduct the same simulations for \hat{q}_n^{VACLE} and \hat{q}_n^{TVACLE} as those with the known σ^2 , but we do not report the results of \hat{q}_n^{PY} with the unknown σ^2 because we found that the results and conclusions are very similar.

Numerical Performance for Known σ^2 Case

Table 3: Mean, mean square error and misestimation rates of \hat{q}_n^{PY} , \hat{q}_n^{VACLE} and \hat{q}_n^{TVACLE} over 500 independent replications for Models 1-3, with known $\sigma^2 = 1$.

	(p, n)	\hat{q}_n^{PY}			\hat{q}_n^{VACLE}			\hat{q}_n^{TVACLE}		
		Mean	MSE	$\hat{q}_n^{PY} \neq q$	Mean	MSE	$\hat{q}_n^{VACLE} \neq q$	Mean	MSE	$\hat{q}_n^{TVACLE} \neq q$
Model 1	(50, 200)	5.022	0.022	0.022	5.004	0.004	0.004	5.024	0.024	0.024
	(200, 800)	5.012	0.012	0.012	5.002	0.002	0.002	5.016	0.016	0.016
	(100, 100)	5.016	0.02	0.02	4.97	0.046	0.046	4.998	0.002	0.002
	(200, 200)	5.026	0.03	0.024	5.01	0.01	0.01	5.004	0.004	0.004
	(100, 50)	4.846	0.218	0.212	4.484	1.296	0.41	4.782	0.222	0.216
	(200, 100)	4.99	0.074	0.074	4.758	0.486	0.194	4.954	0.046	0.046
Model 2	(50, 200)	4.018	0.058	0.028	4.006	0.006	0.006	4.016	0.016	0.016
	(200, 800)	4.016	0.02	0.014	4.004	0.004	0.004	4.032	0.04	0.028
	(100, 100)	3.922	0.246	0.074	3.416	2.112	0.22	3.968	0.036	0.036
	(200, 200)	4.014	0.014	0.014	3.92	0.304	0.048	4.006	0.006	0.006
	(200, 100)	3.558	0.83	0.342	2.452	5.144	0.584	3.712	0.304	0.28
	(400, 200)	3.906	0.162	0.118	3.046	3.138	0.364	3.958	0.05	0.044
Model 3	(50, 200)	3.994	0.118	0.032	3.772	0.804	0.08	4.024	0.024	0.024
	(200, 800)	4.018	0.018	0.018	4	0	0	4.036	0.036	0.036
	(200, 200)	3.456	0.92	0.414	1.94	6.684	0.734	3.614	0.518	0.326
	(400, 400)	3.904	0.18	0.122	2.7	4.152	0.478	3.898	0.142	0.112
	(400, 200)	2.222	3.81	0.952	1.08	9.736	0.968	2.648	2.296	0.91
	(800, 400)	2.626	2.482	0.844	1.588	7.104	0.954	3.022	1.558	0.7

From Table 3, we have the following observations. For Model 1, all three methods work well with high accuracies and small MSE in the cases where the dimension p is smaller than n ($c = p/n = 0.25$). When either $c = 1$ or $c = 2$, \hat{q}_n^{TVACLE} is the best, and \hat{q}_n^{PY} also has smaller MSEs than \hat{q}_n^{VACLE} . In a word, all three methods perform in a satisfactory

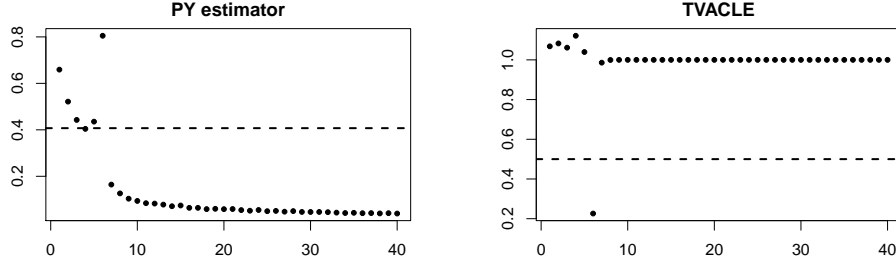
manner, but the performance of \hat{q}_n^{TVACLE} is the most stable for various ratio of $c = p/n$. For Model 2, \hat{q}_n^{VACLE} is sensitive to the ratio c , particularly its MSE. Although when $c = 2$, \hat{q}_n^{TVACLE} may sometimes slightly underestimate the true number, it is less serious than \hat{q}_n^{PY} . For Model 3 with two equal spikes, \hat{q}_n^{TVACLE} works much better than both \hat{q}_n^{PY} and \hat{q}_n^{VACLE} that underestimate q significantly.

Table 4: Mean, mean squared error and empirical distribution of \hat{q}_n^{PY} and \hat{q}_n^{TVACLE} over 500 independent replications for Model 4 ($q = 6$), with known $\sigma^2 = 1$.

	(p, n)	Mean	MSE	$\hat{q} = 0$	$\hat{q} = 1$	$\hat{q} = 2$	$\hat{q} = 3$	$\hat{q} = 4$	$\hat{q} = 5$	$\hat{q} = 6$	$\hat{q} \geq 7$
\hat{q}_n^{PY}	(50, 200)	5.358	2.874	0.018	0.04	0.042	0.06	0	0	0.826	0.014
	(200, 800)	5.816	0.868	0.002	0.014	0.02	0.012	0	0	0.94	0.012
	(100, 100)	4.436	6.904	0.06	0.072	0.118	0.106	0.01	0.048	0.572	0.014
	(200, 200)	4.964	4.772	0.042	0.052	0.082	0.07	0	0	0.742	0.012
	(400, 200)	3.858	9.794	0.078	0.138	0.164	0.094	0.008	0.032	0.484	0.002
	(800, 400)	4.406	7.558	0.068	0.11	0.098	0.086	0	0	0.626	0.012
\hat{q}_n^{TVACLE}	(50, 200)	6.006	0.006	0	0	0	0	0	0	0.994	0.006
	(200, 800)	6.024	0	0	0	0	0	0	0	0.976	0.024
	(100, 100)	5.886	0.122	0	0	0	0	0.004	0.106	0.89	0.11
	(200, 200)	6	0	0	0	0	0	0	0	1	0
	(400, 200)	5.952	0.06	0	0	0	0	0.004	0.042	0.952	0.002
	(800, 400)	6.002	0.002	0	0	0	0	0	0	0.998	0.002

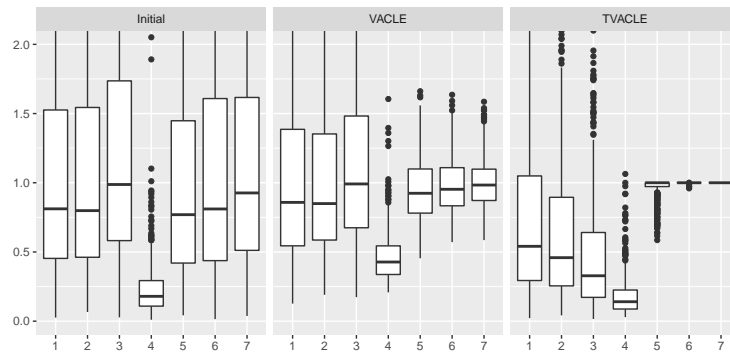
To further confirm this phenomenon, we report the results for Model 4 with more equal spikes. The results in Table 4 suggest that \hat{q}_n^{TVACLE} overall performs better than \hat{q}_n^{PY} in terms of estimation accuracy and MSE, It has underestimation problem as its searching procedure stops earlier once the difference between consecutive eigenvalues corresponding to equal spikes are below the threshold d_n . This conclusion can be made after observing its empirical distributions in Table 4. In contrast, \hat{q}_n^{TVACLE} largely avoids this problem. To better illustrate this fact, we plot in Figure 1 the first 40 differences $\hat{\delta}_i$ for \hat{q}_n^{PY} and the first 40 ratios of \hat{r}_i^{TR} for \hat{q}_n^{TVACLE} . The left subfigure shows that there are three $\hat{\delta}_i$, $i = 3, 4, 5$, are very close to the threshold line $y = d_n$, which causes the underestimation problem shown in Table 4. In contrast, the right subfigure shows that the “valley” \hat{r}_q^{TR} and the “cliff” \hat{r}_{q+1}^{TR} are well separated by the threshold line $\tau = 0.5$.

Figure 1: Plots of the first 40 differences and ratios: the left is for differences $\hat{\delta}_i$, $1 \leq i \leq 40$, in \hat{q}_n^{PY} ; the right is for ratios \hat{r}_i^{TR} , $1 \leq i \leq 40$, in \hat{q}_n^{TVACLE} . The results are based on simulations for Model 4 with 500 independent replications, and $(p, n) = (400, 200)$.



As we claimed in Sections 2 and 3, the VACLE could be somehow sensitive to the ridge selection. The results reported in Table 3 confirm this claim. To explore the manner how the ridge c_n affects both the VACLE and the TVACLE, Figure 2 presents, for Model 2 with $(p, n) = (400, 200)$, the boxplots of the first 7 ratios without ridge \hat{r}_i ; the first 7 ridge ratios \hat{r}_i^R ; and the first 7 transformed ridge ratios \hat{r}_i^{TR} . From the left to right subfigure of Figure 2, we can see that for $i > q = 4$, \hat{r}_i fluctuates much more than \hat{r}_i^R and \hat{r}_4^{TR} and \hat{r}_i^{TR} , $i > 4$ are separated more significantly. This confirms the necessity of using a ridge with a stabilised ratio \hat{r}_i^R and transformation can enhance the estimation accuracy.

Figure 2: Boxplots of the first 7 ratios: the left is for ratios without ridge, \hat{r}_i ; the middle is for ratios with ridge \hat{r}_i^R ; the right is for transformed ratios with ridge \hat{r}_i^{TR} .



The unknown σ^2 Case.

Use Models 2 and 4 and regard σ^2 as an unknown value. These two models represent the cases with and without equal spikes. Furthermore, because the conclusions are very similar to those with known σ^2 , we then report only the results for \hat{q}_n^{VACLE} and \hat{q}_n^{TVACLE} to further confirm the advantages of \hat{q}_n^{TVACLE} . The numerical results are shown in Table 5. The results in the last two columns show that the one-step estimation $\hat{\sigma}^2$ has good performance in terms of accuracy and robustness.

Table 5: Mean and mean square error of \hat{q}_n^{VACLE} , \hat{q}_n^{TVACLE} and $\hat{\sigma}^2$, and the misestimation rates of \hat{q}_n^{VACLE} and \hat{q}_n^{TVACLE} over 500 independent replications for Model 2 and 4, with unknown σ^2 whose true value is 1.

	(p, n)	\hat{q}_n^{VACLE}			\hat{q}_n^{TVACLE}			$\hat{\sigma}^2$	
		Mean	MSE	$\hat{q}_n^{VACLE} \neq q$	Mean	MSE	$\hat{q}_n^{TVACLE} \neq q$	Mean	MSE
Model 2	(50, 200)	4.002	0.002	0.002	4.012	0.012	0.012	1.0513	0.0033
	(200, 800)	4.002	0.002	0.002	4.014	0.014	0.014	1.0119	0.0002
	(100, 100)	3.326	2.346	0.258	3.966	0.038	0.038	1.0326	0.0022
	(200, 200)	3.96	0.176	0.04	4.006	0.006	0.006	1.0169	0.0006
	(200, 100)	2.334	5.726	0.616	3.71	0.306	0.282	1.0205	0.0008
	(400, 200)	3.266	2.454	0.292	3.962	0.038	0.038	1.0094	0.0002
Model 4	(50, 200)	6.01	0.01	0.01	6.01	0.01	0.01	1.0788	0.0069
	(200, 800)	6.002	0.002	0.002	6.022	0.022	0.022	1.0181	0.0004
	(100, 100)	4.082	10.362	0.388	5.878	0.142	0.112	1.0555	0.0042
	(200, 200)	5.846	0.938	0.034	6	0	0	1.0256	0.0009
	(400, 200)	4.524	8.064	0.306	5.958	0.042	0.042	1.0165	0.0004
	(800, 400)	5.822	0.966	0.034	6.01	0.01	0.01	1.0079	9×10^{-5}

5.3 Numerical studies on large dimensional auto-covariance matrix

To estimate the number of factors in Model (4.8), Li et al. (2017) introduced the following ratio-based estimator,

$$\hat{q}_T^{LWY} = \min\{i \geq 1 : \hat{\lambda}_{i+1}/\hat{\lambda}_i > 1 - d_T \text{ and } \hat{\lambda}_{i+2}/\hat{\lambda}_{i+1} > 1 - d_T\} - 1, \quad (5.4)$$

where $\hat{\lambda}_i, 1 \leq i \leq p$, are in descending order and d_T is a tuning parameter selected as that in Section 3.1 of Li et al. (2017). To examine the performance of the \hat{q}_n^{TVACLE} , we use

\hat{q}_T^{LWY} as the competitor. For the ratio $p/T = y$, we consider two values $y = 0.5$ and $y = 2$. The dimension $p = 100, 200, 300, 400$ and 500 . In each case, we repeat the experiment 500 times. To be fair and concise, we conduct the simulation with two models as follows. The model structure is the same as in [Lam and Yao \(2012\)](#) and [Li et al. \(2017\)](#): for $1 \leq t \leq T$

$$y_t = \mathbf{A}x_t + \varepsilon_t, \varepsilon_t \sim \mathbb{N}_p(\mathbf{0}, \mathbf{I}_p), x_t = \Theta x_{t-1} + e_t, e_t \sim \mathbb{N}_k(\mathbf{0}, \Gamma), \quad (5.5)$$

where $\mathbf{A} \in \mathbb{R}^{p \times q}$ is the factor loading matrix and $\{\varepsilon_t\}$ is a white noise sequence with unit variance $\sigma^2 = 1$. As in [Li et al. \(2017\)](#), \mathbf{A} and Γ take the forms as $\mathbf{A} = (\mathbf{I}_q, \mathbf{O}_{(p-q) \times q})^\top$, $\Gamma = \text{diag}(2, 2, \dots, 2)$. We manipulate the strength of factors by adjusting the matrix Θ in different models as follows:

Model 5. *This model is the same as Scenario III in [Li et al. \(2017\)](#). There are $q = 3$ factors whose theoretical limits equal $(7.726, 5.496, 3.613)$ in the case of $y = 0.5$ and $(23.744, 20.464, 17.970)$ in the case of $y = 2$. The upper edge b_1 of the supports in these two cases are respectively 2.773 and 17.637 . $q = 3$ factors are identifiable, and $\Theta = \text{diag}(0.6, -0.5, 0.3)$.*

Model 6. *This model has more factors. There are $q = 6$ factors with identical strength, and their theoretical limits are 5.496 in the case of $y = 0.5$ and 20.464 in the case of $y = 2$. Because these limits exceed their corresponding upper edge b_1 , all $q = 6$ factors are identifiable in theory with $\Theta = \text{diag}(0.5, 0.5, 0.5, 0.5, 0.5, 0.5)$.*

All parameters in the simulations share the same settings of parameters in [Section 5.2](#) where we conduct numerical studies for spiked population models. These parameters in TVACLE estimator are shown in [Table 6](#).

Table 6: Parameters in the TVACLE estimator.

τ	c_T	κ_T	k_1	k_2	L
0.5	$\sqrt{\log \log T} \cdot [q_{p,T}(0.95) - q_{p,T}(0.05)] - m_{p,T}$	$\log \log p \cdot p^{-2/3}$	5	5	20

Table 7: Mean, mean squared error and empirical distribution of \hat{q}_T^{LWY} and \hat{q}_T^{TVACLE} over 500 independent replications for Model 5.

	p	100	200	300	400	500	p	100	200	300	400	500
	$T = 2p$	200	400	600	800	1000		$T = 0.5p$	50	100	150	200
\hat{q}_T^{LWY}	$\hat{q} = 0$	0.024	0.002	0	0	0	$\hat{q} = 0$	0.53	0.238	0.234	0.138	0.054
	$\hat{q} = 1$	0.028	0	0	0	0	$\hat{q} = 1$	0.326	0.412	0.38	0.36	0.282
	$\hat{q} = 2$	0.384	0.138	0.05	0.014	0.008	$\hat{q} = 2$	0.136	0.32	0.356	0.464	0.572
	$\hat{q} = 3$	0.544	0.85	0.948	0.976	0.986	$\hat{q} = 3$	0.008	0.03	0.03	0.036	0.092
	$\hat{q} \geq 4$	0.02	0.01	0.002	0.01	0.006	$\hat{q} \geq 4$	0	0	0	0.002	0
	Mean	2.508	2.866	2.952	2.996	2.998	Mean	0.622	1.142	1.182	1.404	1.702
	MSE	0.732	0.166	0.052	0.024	0.014	MSE	6.21	4.11	3.982	3.148	2.186
\hat{q}_T^{TVACLE}	$\hat{q} = 0$	0	0	0	0	0	$\hat{q} = 0$	0.02	0.002	0	0.002	0
	$\hat{q} = 1$	0	0	0	0	0	$\hat{q} = 1$	0.332	0.182	0.116	0.104	0.054
	$\hat{q} = 2$	0.196	0.02	0.014	0.008	0.002	$\hat{q} = 2$	0.584	0.698	0.688	0.73	0.676
	$\hat{q} = 3$	0.782	0.948	0.974	0.964	0.974	$\hat{q} = 3$	0.062	0.116	0.196	0.16	0.268
	$\hat{q} \geq 4$	0.022	0.032	0.012	0.028	0.024	$\hat{q} \geq 4$	0.002	0.002	0	0.004	0.002
	Mean	2.826	3.012	2.998	3.02	3.022	Mean	1.694	1.934	2.08	2.06	2.218
	MSE	0.218	0.052	0.026	0.036	0.026	MSE	2.094	1.446	1.152	1.168	0.894

Table 8: Mean, mean squared error and empirical distribution of \hat{q}_T^{LWY} and \hat{q}_T^{TVACLE} over 500 independent replications for Model 6.

	p	100	200	300	400	500	p	100	200	300	400	500
	$T = 2p$	200	400	600	800	1000		$T = 0.5p$	50	100	150	200
\hat{q}_T^{LWY}	$\hat{q} = 0$	0.156	0.104	0.072	0.098	0.054	$\hat{q} = 0$	0.226	0.202	0.26	0.24	0.134
	$\hat{q} = 1$	0.178	0.154	0.124	0.146	0.076	$\hat{q} = 1$	0.418	0.35	0.326	0.304	0.28
	$\hat{q} = 2$	0.19	0.154	0.114	0.104	0.062	$\hat{q} = 2$	0.296	0.314	0.262	0.236	0.312
	$\hat{q} = 3$	0.162	0.112	0.068	0.106	0.044	$\hat{q} = 3$	0.06	0.122	0.134	0.17	0.188
	$\hat{q} = 4$	0.13	0.006	0	0	0	$\hat{q} = 4$	0	0.012	0.016	0.05	0.07
	$\hat{q} = 5$	0.112	0.072	0	0	0	$\hat{q} = 5$	0	0	0.002	0	0.014
	$\hat{q} = 6$	0.072	0.394	0.62	0.542	0.754	$\hat{q} = 6$	0	0	0	0	0.002
	$\hat{q} \geq 7$	0	0.004	0.002	0.004	0.01	$\hat{q} \geq 7$	0	0	0	0	0
	Mean	2.556	3.574	4.29	3.954	4.926	Mean	1.19	1.392	1.326	1.486	1.83
MSE	15.196	11.166	8.13	9.806	5.242	MSE	23.862	22.192	22.974	21.746	18.802	
\hat{q}_T^{TVACLE}	$\hat{q} = 0$	0	0	0	0	0	$\hat{q} = 0$	0	0	0	0	0
	$\hat{q} = 1$	0	0	0	0	0	$\hat{q} = 1$	0.01	0	0	0	0
	$\hat{q} = 2$	0	0	0	0	0	$\hat{q} = 2$	0.206	0.07	0.03	0.008	0.008
	$\hat{q} = 3$	0.004	0	0	0	0	$\hat{q} = 3$	0.586	0.496	0.33	0.224	0.13
	$\hat{q} = 4$	0.066	0.002	0	0	0	$\hat{q} = 4$	0.19	0.414	0.546	0.574	0.554
	$\hat{q} = 5$	0.418	0.038	0	0	0	$\hat{q} = 5$	0.008	0.02	0.094	0.188	0.294
	$\hat{q} = 6$	0.51	0.946	0.99	0.984	0.97	$\hat{q} = 6$	0	0	0	0.006	0.014
	$\hat{q} \geq 7$	0.002	0.014	0.01	0.016	0.03	$\hat{q} \geq 7$	0	0	0	0	0
	Mean	5.44	5.972	6.01	6.016	6.03	Mean	2.98	3.384	3.704	3.96	4.176
MSE	0.72	0.06	0.01	0.016	0.03	MSE	9.588	7.26	5.728	4.628	3.808	

From Table 7, we can see that when $T = 2p$, \hat{q}_T^{LWY} works well. That is, when T is large,

\hat{q}_T^{LWY} shows good performance, whilst when T is not large, it tends to underestimate the true number q . Our method clearly outperforms \hat{q}_T^{LWY} . Although when T is small, the true value is somewhat underestimated, but still, with high proportion, to be two or greater. Table 8 shows that for Model 6 with equal spikes, when $T = 2p$, the performance of \hat{q}_T^{LWY} is not encouraging, and when $T = 0.5p$, the underestimation problem becomes very serious, with a very high proportion having $\hat{q}_T^{LWY} \leq 2$. In contrast, our method performs well when $T = 2p$ and when $T = 0.5p$; underestimation still occurs, but it is much less serious than \hat{q}_T^{LWY} in the sense that $\hat{q} > 2$ with high proportion. Overall, our estimator \hat{q}_T^{TVACLE} is superior to \hat{q}_T^{LWY} in these limited simulations.

5.4 Numerical studies on large dimensional spiked Fisher matrix

Because the TVACLE has been demonstrated to outperform the VACLE overall, we only consider the comparison between \hat{q}_n^{TVACLE} and the estimator \hat{q}_n^{WY} introduced by Wang and Yao (2017). Sharing notations in Section 4, the estimator \hat{q}_n^{WY} can be written as

$$\hat{q}_n^{WY} = \max\{i : \hat{\lambda}_i \geq b_2 + d_n\}, \quad (5.6)$$

where d_n was recommended to be $(\log \log p)p^{-2/3}$ in their paper.

As a Fisher matrix $\mathbf{F}_n = \mathbf{S}_1 \mathbf{S}_2^{-1}$ involves two random matrices \mathbf{S}_1 and \mathbf{S}_2 , its eigenvalues are more dispersed, with wider range of the support, than the spiked sample covariance matrices and auto-covariance matrices. The aforementioned automatic procedure for ridge selection would then generate a larger c_n , and this in turn increases the value at the “valley”. Hence, we use a larger threshold $\tau = 0.8$ to avoid underestimation. Further, in the following Model 7, we set the ridge $c_n^{(3)} = \sqrt{\log \log p} \cdot [q_{p,n}(0.95) - q_{p,n}(0.05)] - m_{p,n}$, whilst for Model 8 with dramatically-fluctuated extreme eigenvalues, we need to set $c_n^{(3)} = \sqrt{\log \log p} \cdot [q_{p,n}(0.8) - q_{p,n}(0.05)] - m_{p,n}$ to avoid too large ridge. The parameters in \hat{q}_n^{TVACLE} are shown in Table 9.

Again, for a fair comparison, we design two models, one that was used by Wang and Yao (2017) and the other with weaker spikes. For $y = p/T$ and $c = p/n$, we set (0.5, 0.2)

Table 9: Parameters in the TVACLE estimator.

τ	c_n	κ_n	k_1	k_2	L
0.8	$c_n^{(3)}$	$\log \log p \cdot p^{-2/3}$	5	5	20

and (0.2, 0.5) for the respective models. The dimension p takes values of 50, 100, 150, 200 and 250. For each combination (p, T, n) , the experiment is repeated 500 times. Consider the number of spikes to be $q = 3$ and \mathbf{A} to be a $p \times 3$ matrix as:

$$\begin{pmatrix} \sqrt{\alpha_1} & 0 & 0 & 0 & \cdots & 0 \\ 0 & \sqrt{\frac{\alpha_2}{2}} & \sqrt{\frac{\alpha_2}{2}} & 0 & \cdots & 0 \\ 0 & \sqrt{\frac{\alpha_3}{2}} & -\sqrt{\frac{\alpha_3}{2}} & 0 & \cdots & 0 \end{pmatrix}_{3 \times p}^T, \quad (5.7)$$

where $\alpha = (\alpha_1, \alpha_2, \alpha_3)$ assumes different values in two models. Assume the covariance matrix $Cov(u_i) = \mathbf{I}_3$ and $\Sigma_2 = \text{diag}(1, \dots, 1, 2, \dots, 2)$, where “1” and “2” both have multiplicity $p/2$. The two models are:

Model 7. Let $\alpha = (10, 5, 5)$, $(y, c) = (0.5, 0.2)$, which is Model 1 in Wang and Yao (2017). The matrix $\Sigma_1 \Sigma_2^{-1}$ has three spikes $\lambda_1 = 11$ and $\lambda_2 = \lambda_2 = 6$ that are all significantly larger than the upper bound $b_2 = \frac{1 + \sqrt{c+y-cy}}{1-y} \approx 3.55$ of support of the distribution.

Model 8. Let $\alpha = (10, 2, 2)$, $(y, c) = (0.2, 0.5)$. The matrix $\Sigma_1 \Sigma_2^{-1}$ then also has three spikes $\lambda_1 = 11$ and $\lambda_2 = \lambda_2 = 3$ larger than the upper bound $b_2 = \frac{1 + \sqrt{c+y-cy}}{1-y} \approx 2.22$ of the support of the distribution. Then $\lambda_2 = \lambda_2 = 3$ are relatively more difficult to detect.

Table 10: Mean, mean squared error and empirical distribution of \hat{q}_n^{WY} and \hat{q}_n^{TVACLE} for Model 7.

	(p, T, n)	Mean	MSE	$\hat{q} = 0$	$\hat{q} = 1$	$\hat{q} = 2$	$\hat{q} = 3$	$\hat{q} = 4$
\hat{q}_n^{WY}	(50, 100, 250)	2.344	0.732	0	0.034	0.592	0.37	0.004
	(100, 200, 500)	2.672	0.352	0	0.004	0.328	0.66	0.008
	(150, 300, 750)	2.822	0.194	0	0	0.186	0.806	0.008
	(200, 400, 1000)	2.964	0.092	0	0	0.064	0.908	0.028
	(250, 500, 1250)	2.96	0.068	0	0	0.054	0.932	0.014
\hat{q}_n^{TVACLE}	(50, 100, 250)	2.364	0.7	0	0.028	0.584	0.384	0.004
	(100, 200, 500)	2.688	0.336	0	0.004	0.312	0.676	0.008
	(150, 300, 750)	2.842	0.182	0	0	0.17	0.818	0.012
	(200, 400, 1000)	2.974	0.082	0	0	0.054	0.918	0.028
	(250, 500, 1250)	2.964	0.064	0	0	0.05	0.936	0.014

Table 11: Mean, mean squared error and empirical distribution of \hat{q}_n^{WY} and \hat{q}_n^{TVACLE} for Model 8.

	(p, T, n)	Mean	MSE	$\hat{q} = 0$	$\hat{q} = 1$	$\hat{q} = 2$	$\hat{q} = 3$	$\hat{q} = 4$
\hat{q}_n^{WY}	(50, 250, 100)	2.114	1.07	0	0.09	0.708	0.2	0.002
	(100, 500, 200)	2.302	0.79	0	0.046	0.606	0.348	0
	(150, 750, 300)	2.498	0.538	0	0.018	0.466	0.516	0
	(200, 1000, 400)	2.622	0.394	0	0.006	0.368	0.624	0.002
	(250, 1250, 500)	2.692	0.324	0	0.004	0.304	0.688	0.004
\hat{q}_n^{TVACLE}	(50, 250, 100)	2.238	0.898	0	0.064	0.638	0.294	0.004
	(100, 500, 200)	2.462	0.602	0	0.03	0.48	0.488	0.002
	(150, 750, 300)	2.71	0.314	0	0	0.302	0.686	0.012
	(200, 1000, 400)	2.82	0.232	0	0.002	0.2	0.774	0.024
	(250, 1250, 500)	2.904	0.164	0	0	0.13	0.836	0.034

The results reported in Tables 10 and 11 show that \hat{q}_n^{TVACLE} shows overall better performance than \hat{q}_n^{WY} . For Model 8, \hat{q}_n^{TVACLE} is superior to \hat{q}_n^{WY} when the signals are relatively weak.

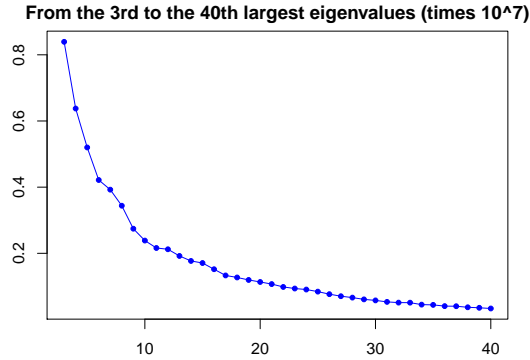
6 Real data example

Consider a data set of the daily prices of 100 stocks (see Li et al. (2017)). This dataset includes the stock prices of the S&P500 from 2005-01-03 to 2006-12-29. Except for incomplete data, every stock has 502 observations of log returns. Thus, $T = 502$, $p = 100$, and then $c = p/T \approx 0.2$.

Denote $y_t \in \mathbb{R}^p$, $1 \leq t \leq T$, as the t -th observation of the log return of these 100 stocks, and we then obtain its lag-1 sample auto-covariance matrix $\hat{\Sigma}_y$ and the matrix $\hat{\mathbf{M}}_y = \hat{\Sigma}_y \hat{\Sigma}_y^\top$ as formulated in Section 4. Use \hat{q}_n^{TVACLE} and \hat{q}_n^{LWY} in Li et al. (2017) to determine the number of factors. All parameters in these two methods share the same settings. We can see that the two largest eigenvalues of $\hat{\mathbf{M}}_y$ are 7.17×10^{-7} and 2.01×10^{-7} , and the third to the 40-th eigenvalues are shown in Figure 3.

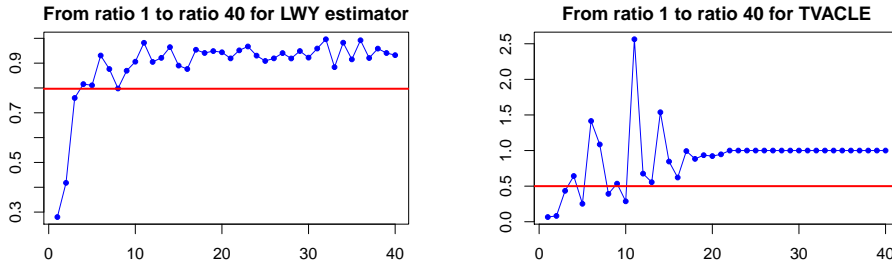
Figure 4 shows that $\hat{q}_n^{LWY} = 5$. However, as shown in Figure 3, the gap between the 5th eigenvalue and several following eigenvalues is evidently insignificant. As \hat{q}_n^{LWY} is based on the magnitudes of the next two consecutive ratios. If eigenvalue multiplicity occurs, \hat{q}_n^{LWY}

Figure 3: Eigenvalues of $\hat{\mathbf{M}}_y$ from $\hat{\lambda}_3$ to $\hat{\lambda}_{40}$



could likely select a value smaller than the true number.

Figure 4: Ratios $\hat{\lambda}_{i+1}/\hat{\lambda}_i$ in Li et al. (2017) and Ratios \hat{r}_i^{TR} in the TVACLE, $1 \leq i \leq 40$.



When the TVACLE is used, $\hat{q}^{TVACLE} = 10$. Figure 4 shows that the 11th ratio is much larger than the 10th ratio, although some values get smaller. Note that in this example, $c \sim 0.2$ and the ridge is relatively small, which would not very much dominate the difference between the eigenvalues and thus some oscillating values remain after the 10th ratio.

It is considered that \hat{q}^{LWY} would neglect several factors and likely result in an underestimation. For a real data example, we usually cannot give a definitive answer. However, our method could provide an estimation that would be relatively conservative but necessary, particularly in the initial stage of data analysis; otherwise, an excessively parsimonious model would cause misleading conclusions.

7 Concluding remarks

In this paper, we propose a valley-cliff criterion for spiked models, and the method can be applied to other order determination problems when the dimension is proportional to the sample size, such as those in sufficient dimension reduction if the corresponding asymptotics can be well investigated. The method is for the case with a fixed order q . An extension to the case with diverging q will be proposed in our future work.

Supplementary Materials

Proofs and technical details are contained in the supplementary materials.

References

- Baik, J., G. B. Arous, and S. Péché (2005). Phase transition of the largest eigenvalue for nonnull complex sample covariance matrices. *The Annals of Probability* 33(5), 1643–1697.
- Baik, J. and J. W. Silverstein (2006). Eigenvalues of large sample covariance matrices of spiked population models. *Journal of Multivariate Analysis* 97(6), 1382–1408.
- Bao, Z., G. Pan, and W. Zhou (2015). Universality for the largest eigenvalue of sample covariance matrices with general population. *The Annals of Statistics* 43(1), 382–421.
- Benaych-Georges, F., A. Guionnet, and M. Maida (2011). Fluctuations of the extreme eigenvalues of finite rank deformations of random matrices. *Electronic Journal of Probability* 16(60), 1621–1662.
- Benaych-Georges, F. and R. R. Nadakuditi (2011). The eigenvalues and eigenvectors of finite, low rank perturbations of large random matrices. *Advances in Mathematics* 227(1), 494–521.

- Han, X., G. Pan, and Q. Yang (2018). A unified matrix model including both CCA and F matrices in multivariate analysis: the largest eigenvalue and its applications. *Bernoulli* 24(4B), 3447–3468.
- Han, X., G. Pan, and B. Zhang (2016). The tracy–widom law for the largest eigenvalue of F type matrices. *The Annals of Statistics* 44(4), 1564–1592.
- Johnstone, I. M. (2001). On the distribution of the largest eigenvalue in principal components analysis. *The Annals of Statistics* 29(2), 295–327.
- Johnstone, I. M. and A. Y. Lu (2009). On consistency and sparsity for principal components analysis in high dimensions. *Journal of the American Statistical Association* 104(486), 682–693.
- Knowles, A. and J. Yin (2017). Anisotropic local laws for random matrices. *Probability Theory and Related Fields* 169(1-2), 257–352.
- Kritchman, S. and B. Nadler (2008). Determining the number of components in a factor model from limited noisy data. *Chemometrics and Intelligent Laboratory Systems* 94(1), 19–32.
- Lam, C. and Q. Yao (2012). Factor modeling for high-dimensional time series: inference for the number of factors. *The Annals of Statistics* 40(2), 694–726.
- Li, K.-C. (1991). Sliced inverse regression for dimension reduction. *Journal of the American Statistical Association* 86(414), 316–327.
- Li, Z., Q. Wang, and J. Yao (2017). Identifying the number of factors from singular values of a large sample auto-covariance matrix. *The Annals of Statistics* 45(1), 257–288.
- Luo, W. and B. Li (2016). Combining eigenvalues and variation of eigenvectors for order determination. *Biometrika* 103(4), 875–887.

- Nadler, B. (2010). Nonparametric detection of signals by information theoretic criteria: performance analysis and an improved estimator. *IEEE Transactions on Signal Processing* 58(5), 2746–2756.
- Onatski, A. (2009). Testing hypotheses about the number of factors in large factor models. *Econometrica* 77(5), 1447–1479.
- Passemier, D., Z. Li, and J. Yao (2017). On estimation of the noise variance in high dimensional probabilistic principal component analysis. *Journal of the Royal Statistical Society: Series B (Statistical Methodology)* 79(1), 51–67.
- Passemier, D. and J. Yao (2012). On determining the number of spikes in a high-dimensional spiked population model. *Random Matrices: Theory and Applications* 1(01), 1150002.
- Passemier, D. and J. Yao (2014). Estimation of the number of spikes, possibly equal, in the high-dimensional case. *Journal of Multivariate Analysis* 127, 173–183.
- Péché, S. (2006). The largest eigenvalue of small rank perturbations of hermitian random matrices. *Probability Theory and Related Fields* 134(1), 127–173.
- Pillai, N. S. and J. Yin (2014). Universality of covariance matrices. *The Annals of Applied Probability* 24(01), 935–1001.
- Ulfarsson, M. O. and V. Solo (2008). Dimension estimation in noisy pca with sure and random matrix theory. *IEEE Transactions on Signal Processing* 56(12), 5804–5816.
- Wang, Q. and J. Yao (2017). Extreme eigenvalues of large-dimensional spiked fisher matrices with application. *The Annals of Statistics* 45(1), 415–460.
- Xia, Q., W. Xu, and L. Zhu (2015). Consistently determining the number of factors in multivariate volatility modelling. *Statistica Sinica* 25(3), 1025–1044.
- Zhu, L., B. Miao, and H. Peng (2006). On sliced inverse regression with high-dimensional covariates. *Journal of the American Statistical Association* 101(474), 630–643.

Zhu, L., T. Wang, L. Zhu, and L. Ferré (2010). Sufficient dimension reduction through discretization-expectation estimation. *Biometrika* 97(2), 295–304.

Yicheng Zeng, Department of Mathematics, Hong Kong Baptist University, Hong Kong

E-mail: statzyc@163.com

Lixing Zhu, Department of Mathematics, Hong Kong Baptist University, Hong Kong

E-mail: lzhu@hkbu.edu.hk

Supplementary Materials for “Order Determination for Spiked Models”

Yicheng Zeng and Lixing Zhu

Department of Mathematics, Hong Kong Baptist University, Hong Kong

Proof of Theorem 2.1 We only need to check that

$$\lim_{n \rightarrow +\infty} \mathbb{P} \left(\frac{\hat{\delta}_{i+1} + \sigma^2 c_n}{\hat{\delta}_i + \sigma^2 c_n} > \tau \right) = 1, \text{ for } q < i \leq L - 2, \quad (7.1)$$

and

$$\lim_{n \rightarrow +\infty} \mathbb{P} \left(\frac{\hat{\delta}_{q+1} + \sigma^2 c_n}{\hat{\delta}_q + \sigma^2 c_n} \leq \tau \right) = 1. \quad (7.2)$$

For any $q < i \leq L - 2$, we have in probability

$$\frac{\hat{\delta}_{i+1} + \sigma^2 c_n}{\hat{\delta}_i + \sigma^2 c_n} = \frac{\hat{\delta}_{i+1}/\sigma^2 + c_n}{\hat{\delta}_i/\sigma^2 + c_n} \rightarrow 1 > \tau, \quad (7.3)$$

as $\hat{\delta}_{i+1}/\sigma^2 = O_p(\tilde{c}_n)$ and $\tilde{c}_n = o(c_n)$. Thus, $\mathbb{P}(\frac{\hat{\delta}_{i+1} + \sigma^2 c_n}{\hat{\delta}_i + \sigma^2 c_n} > \tau) \rightarrow 1$, for $q < i \leq L - 2$.

Further, in probability

$$\frac{\hat{\delta}_{q+1} + \sigma^2 c_n}{\hat{\delta}_q + \sigma^2 c_n} = \frac{\hat{\delta}_{q+1}/\sigma^2 + c_n}{\hat{\delta}_q/\sigma^2 + c_n} = \frac{o_p(1) + c_n}{d - e + o_p(1) + c_n} \rightarrow 0 < \tau, \quad (7.4)$$

as $d - e > 0$. Thus, $\mathbb{P}(\frac{\hat{\delta}_{q+1} + \sigma^2 c_n}{\hat{\delta}_q + \sigma^2 c_n} \leq \tau) \rightarrow 1$. Therefore, the result is proved. \square

Proof of Lemma 3.1. Firstly, we check the requirement (i). As f_n is differentiable, $\exists \xi_q \in (\hat{\lambda}_{q+1}/\sigma^2, \hat{\lambda}_q/\sigma^2)$, s.t.

$$\hat{\delta}_q^* = f_n(\hat{\lambda}_q/\sigma^2) - f_n(\hat{\lambda}_{q+1}/\sigma^2) = f'_n(\xi_q) \hat{\delta}_q. \quad (7.5)$$

We then only need to check that

$$\mathbb{P}\{f'_n(\xi_q) \geq 1\} \rightarrow 1, \text{ as } n \rightarrow \infty. \quad (7.6)$$

By conditions (b) and (c), it suffices to show that

$$\mathbb{P}\{\xi_q > e - \kappa_n\} \longrightarrow 1, \quad \text{as } n \rightarrow \infty. \quad (7.7)$$

On the other hand, from the definition of κ_n in condition (c), we have

$$\hat{\lambda}_{q+1}/\sigma^2 - e = o_P(\kappa_n), \quad (7.8)$$

which is equivalent to

$$\frac{\hat{\lambda}_{q+1}/\sigma^2 - e}{\kappa_n} = o_P(1). \quad (7.9)$$

Then we have

$$\mathbb{P}\{\xi_q > e - \kappa_n\} \geq \mathbb{P}\left\{\frac{\hat{\lambda}_{q+1}}{\sigma^2} > e - \kappa_n\right\} = \mathbb{P}\left\{\frac{\hat{\lambda}_{q+1}/\sigma^2 - e}{\kappa_n} > -1\right\} \rightarrow 1. \quad (7.10)$$

(i) is then verified.

Now we check (ii). Similarly, we have

$$\hat{\delta}_i^* = f'(\xi_i)\hat{\delta}_i/\sigma^2, \quad \text{for } q+1 \leq i \leq p-2, \quad (7.11)$$

where $\xi_i \in (\hat{\lambda}_{i+1}/\sigma^2, \hat{\lambda}_i/\sigma^2)$. Then it suffices to show that

$$\mathbb{P}\{\xi_i < e + \kappa_n\} \longrightarrow 1, \quad \text{for } q+1 \leq i \leq p-2. \quad (7.12)$$

Since $\xi_{q+1} > \cdots > \xi_{p-2}$, it is equivalent to

$$\mathbb{P}\{\xi_{q+1} < e + \kappa_n\} \longrightarrow 1, \quad (7.13)$$

whose proof is completely parallel to that of (i).

For (iii), we have

$$\frac{\hat{\delta}_{q+1}^*}{\hat{\delta}_q^*} = \frac{f'_n(\xi_{q+1})\hat{\delta}_{q+1}}{f'_n(\xi_q)\hat{\delta}_q} \quad (7.14)$$

Condition (b) yields

$$f'_n(\xi_{q+1}) \leq f'_n(\xi_q), \quad (7.15)$$

since $\xi_{q+1} < \hat{\lambda}_{q+1}/\sigma^2 < \xi_q$. Therefore,

$$\frac{\hat{\delta}_{q+1}^*}{\hat{\delta}_q^*} \leq \frac{\hat{\delta}_{q+1}}{\hat{\delta}_q}. \quad (7.16)$$

The requirement (iii) is then proved and the proof of the lemma is finished. \square

Proof of Theorem 3.1. Similar to the proof of Theorem 2.1, we only need to check that

$$\lim_{n \rightarrow \infty} \mathbb{P} \left\{ \frac{\hat{\delta}_{i+1}^* + c_n}{\hat{\delta}_i^* + c_n} > \tau \right\} = 1, \quad \text{for } q < i \leq L - 2 \quad (7.17)$$

and

$$\lim_{n \rightarrow \infty} \mathbb{P} \left\{ \frac{\hat{\delta}_{q+1}^* + c_n}{\hat{\delta}_q^* + c_n} \leq \tau \right\} = 1. \quad (7.18)$$

On one hand, since Lemma 3.1 ensures the requirement (ii), for $q < i \leq L - 2$,

$$\hat{\delta}_i^* = o_p(c_n), \quad (7.19)$$

which leads to $\hat{\delta}_i^* c_n^{-1} = o_p(1)$. Then

$$\frac{\hat{\delta}_{i+1}^* + c_n}{\hat{\delta}_i^* + c_n} = \frac{\hat{\delta}_{i+1}^* c_n^{-1} + 1}{\hat{\delta}_i^* c_n^{-1} + 1} = \frac{o_p(1) + 1}{o_p(1) + 1} \xrightarrow{P} 1 > \tau. \quad (7.20)$$

That is,

$$\lim_{n \rightarrow +\infty} \mathbb{P} \left\{ \frac{\hat{\delta}_{i+1}^* + c_n}{\hat{\delta}_i^* + c_n} > \tau \right\} = 1, \quad \text{for } q < i \leq L - 2. \quad (7.21)$$

On the other hand, because of (i), (ii) and

$$\lim_{n \rightarrow +\infty} \mathbb{P} \left\{ \frac{\hat{\delta}_{q+1}/\sigma^2 + c_n}{\hat{\delta}_q/\sigma^2 + c_n} \leq \tau \right\} \rightarrow 1, \quad (7.22)$$

we have

$$\lim_{n \rightarrow +\infty} \mathbb{P} \left\{ \frac{\hat{\delta}_{q+1}^* + c_n}{\hat{\delta}_q^* + c_n} \leq \tau \right\} \rightarrow 1. \quad (7.23)$$

Thus, \hat{q}_n^{TVACLE} is equal to q with a probability going to 1. The proof is concluded. \square

Proof of Theorem 4.1. First, we show that $U(F) = \sigma^2(1 + \sqrt{c})$ is the optimal lower bound we defines in Theorem 2.1. As [Passemier and Yao \(2012\)](#) and [Passemier and Yao \(2014\)](#) pointed out, together with the results with $\sigma^2 = 1$ in [Baik and Silverstein \(2006\)](#), a scale transformation $\hat{\lambda}_i \mapsto (\sigma^2)^{-1}\hat{\lambda}_i$ can derive the results with the general σ^2 as follows. When $0 \leq c \leq 1$, the empirical distribution of all estimated eigenvalues $\hat{\lambda}_i$ almost surely converges to the famous Marcenko-Pastur distribution in the support interval $(\sigma^2(1 - \sqrt{c})^2, \sigma^2(1 + \sqrt{c})^2) := (a, b)$. To be specific,

$$\frac{1}{p} \#\{\hat{\lambda}_i : \hat{\lambda}_i < x\} \rightarrow F_{c, \sigma^2}(x) \quad a.s. \quad (7.24)$$

with the density function

$$F'_{c, \sigma^2}(x) = \frac{1}{2\pi x c \sigma^2} \sqrt{(b-x)(x-a)}, \quad a < x < b. \quad (7.25)$$

When $c > 1$, the integral of the above density function over the interval (a, b) is equal to $1/c$, and there is an additional Dirac measure of mass $1 - \frac{1}{c}$ at the origin $x = 0$. These results show that completely unlike the case with the fixed p , there are the number of the estimated eigenvalues proportional to n larger than σ^2 and thus, using estimated eigenvalues to identify q_1 is impossible. Slightly generalizing the results of [Baik and Silverstein \(2006\)](#), we can also have the phase transition phenomenon for spiked population models: for any fixed L with $q + 3 \leq L < p$,

$$\hat{\lambda}_i \rightarrow \sigma^2 \phi(\lambda_i / \sigma^2) \quad a.s. \quad \forall i \leq q, \quad (7.26)$$

$$\hat{\lambda}_i \rightarrow b \quad a.s., \quad \text{for } q + 1 \leq i \leq L, \quad (7.27)$$

where $q := \#\{\lambda_i : \lambda_i > \sigma^2(1 + \sqrt{c})\}$, and $\phi(x) := x + \frac{cx}{x-1}$ which is a strictly increasing function on $(1 + \sqrt{c}, +\infty)$. That is to say, only q extreme sample eigenvalues would converge to values larger than the right hand end b of the interval (a, b) if their corresponding spikes exceed the value $\sigma^2(1 + \sqrt{c})$. Otherwise, the estiated eigenvalues corresponding to

$\sigma^2 < \lambda_i \leq \sigma^2(1 + \sqrt{c})$ for $q + 1 \leq i \leq L$ converge to the same value b . This causes that these estimated eigenvalues are inseparable from those of $\lambda_i = \sigma^2$.

Further, [Bai and Yao \(2008\)](#) established Central Limit Theorem of $\hat{\lambda}_i$, for $1 \leq i \leq q$ that implies the \sqrt{n} -consistency of $\hat{\lambda}_i$. Combining Proposition 5.8 of [Benaych-Georges et al. \(2011\)](#) and Corollary 1.5 and Remark 1.6 in [Bao et al. \(2015\)](#), we have that, for any fixed integer $L > q + 1$, $\hat{\lambda}_i - b = O_P(n^{-2/3})$ and then $\hat{\delta}_i = O_P(n^{-2/3})$ for $q + 1 \leq i \leq L$, where $b = \sigma^2(1 + \sqrt{c})^2$.

According to the property of $\hat{\lambda}_i$, we have

$$\lim_{n \rightarrow \infty} \hat{\delta}_i = \begin{cases} \sigma^2 \phi(\lambda_i/\sigma^2) - \sigma^2 \phi(\lambda_{i+1}/\sigma^2) \text{ a.s.} & \text{for } 1 \leq i \leq q - 1, \\ \sigma^2 \phi(\lambda_q/\sigma^2) - b > 0 \text{ a.s.} & \text{for } i = q, \\ 0, \text{ a.s.} & \text{for } q + 1 \leq i \leq L - 1. \end{cases} \quad (7.28)$$

Then the ratios have the following valley-cliff property at the index q : if defining $0/0$ as 1,

$$\begin{aligned} \lim_{n \rightarrow \infty} \hat{r}_i &= \lim_{n \rightarrow \infty} \frac{\hat{\delta}_{i+1}}{\hat{\delta}_i} = \begin{cases} \frac{\sigma^2 \phi(\lambda_{i+1}/\sigma^2) - \sigma^2 \phi(\lambda_{i+2}/\sigma^2)}{\sigma^2 \phi(\lambda_i/\sigma^2) - \sigma^2 \phi(\lambda_{i+1}/\sigma^2)}, & \text{for } 1 \leq i \leq q - 2 \\ \frac{\sigma^2 \phi(\lambda_q/\sigma^2) - b}{\sigma^2 \phi(\lambda_{q-1}/\sigma^2) - \sigma^2 \phi(\lambda_q/\sigma^2)}, & \text{for } i = q - 1 \\ 0, & \text{for } i = q \\ 0/0 = 1, & \text{for } q + 1 \leq i \leq L - 2. \end{cases} \\ &= \begin{cases} \frac{\phi(\lambda_{i+1}/\sigma^2) - \phi(\lambda_{i+2}/\sigma^2)}{\phi(\lambda_i/\sigma^2) - \phi(\lambda_{i+1}/\sigma^2)}, & \text{for } 1 \leq i \leq q - 2 \\ \frac{\phi(\lambda_q/\sigma^2) - (1 + \sqrt{c})^2}{\phi(\lambda_{q-1}/\sigma^2) - \phi(\lambda_q/\sigma^2)}, & \text{for } i = q - 1 \\ 0, & \text{for } i = q \\ 0/0 = 1, & \text{for } q + 1 \leq i \leq L - 2. \end{cases} \end{aligned} \quad (7.29)$$

From this result, we can now consider the ridge ratios. Note that $\hat{\delta}_i = O_P(n^{-2/3})$ for $q + 1 \leq i \leq L - 1$ and $\hat{\delta}_i$ for $1 \leq q$, at the rate of order $O_P(n^{-1/2})$, are either consistent to positive constants or to 0 when spikes are equal. Further, as $c_n \rightarrow 0$ and $c_n^{-1}n^{-2/3} = o(1)$,

we can easily see that $\lim_{n \rightarrow +\infty} \hat{r}_q = 0/(\phi(\lambda_q) - b) = 0$ and then $\hat{r}_q^R \rightarrow 0$ in probability. We then still have the valley-cliff property at the index q :

$$\lim_{n \rightarrow \infty} \hat{r}_i^R = \begin{cases} \geq 0, & i < q \\ 0, & i = q \\ 1, & q + 1 \leq i \leq L - 2. \end{cases} \quad (7.30)$$

□

Proof of Theorem 4.2. When $\sigma^2 = 1$, Wang and Yao (2017) provided the limiting spectral distribution (LSD) of the matrix $\mathbf{F}_n = \mathbf{S}_1 \mathbf{S}_2^{-1}$ and established the phase transition phenomenon for those extreme eigenvalues of \mathbf{F}_n . When $0 < c \leq 1$, the empirical spectral distribution (ESD) of \mathbf{F}_n weakly converges to a distribution $F_{c,y}$ with the density function

$$f_{c,y}(x) = \frac{(1-y)\sqrt{(b_1-x)(x-a_1)}}{2\pi x(c+xy)}, \quad a_2 \leq x \leq b_2, \quad (7.31)$$

where $a_2 = (\frac{1-\sqrt{c+y-cy}}{1-y})^2$ and $b_2 = (\frac{1+\sqrt{c+y-cy}}{1-y})^2$. Similarly as that of spiked population models, when $c > 1$, there is an additional probability measure of mass $1 - \frac{1}{c}$ for $F_{c,y}$. Further, they also proved a phase transition phenomenon that almost surely

$$\begin{aligned} \hat{\lambda}_i &\rightarrow \varphi(\lambda_i), & \lambda_i > \gamma(1 + \sqrt{c+y-cy}), \\ \hat{\lambda}_i &\rightarrow b_2, & 1 < \lambda_i \leq \gamma(1 + \sqrt{c+y-cy}), \end{aligned}$$

where $\gamma = \frac{1}{1-y} \in (1, +\infty)$ and $\varphi(x) = \frac{\gamma x(x-1+c)}{x-\gamma}$, $x \neq \gamma$.

Under the general Fisher matrix with the spiked structure

$$\text{spec}(\Sigma_1 \Sigma_2^{-1}) = \{\lambda_1, \lambda_2, \dots, \lambda_{q_1}, \sigma^2, \dots, \sigma^2\}. \quad (7.32)$$

Using the simple transformation $\hat{\lambda}_i \mapsto (\sigma^2)^{-1} \hat{\lambda}_i$, we can similarly achieve the results in the case of $\sigma^2 = 1$. The empirical spectral distribution of \mathbf{F}_n weakly converges to a distribution F_{c,y,σ^2} with the density function

$$f_{c,y,\sigma^2}(x) = \frac{1}{\sigma^2} f_{c,y}\left(\frac{x}{\sigma^2}\right), \quad \sigma^2 a_1 < x < \sigma^2 b_1, \quad (7.33)$$

and the additional point mass $1 - \frac{1}{c}$ at origin $x = 0$ also exists when $c > 1$. The phase transition phenomenon is modified as

$$\begin{aligned}\hat{\lambda}_i &\rightarrow \sigma^2 \varphi(\lambda_i/\sigma^2), & \lambda_i > \sigma^2 \gamma(1 + \sqrt{c + y - cy}), \\ \hat{\lambda}_i &\rightarrow \sigma^2 b_2, & \sigma^2 < \lambda_i \leq \sigma^2 \gamma(1 + \sqrt{c + y - cy}),\end{aligned}$$

where the parameters b_2 , γ and the function φ have the same definitions as those in the case with $\sigma^2 = 1$. Let $q := \#\{\lambda_i : \lambda_i > U(F) = \sigma^2 \gamma(1 + \sqrt{c + y - cy})\}$. According to these results, for any fixed L with $q + 3 < L < p$

$$\begin{aligned}\hat{\lambda}_i &\rightarrow \sigma^2 \varphi(\lambda_i/\sigma^2), & 1 \leq i \leq q, \\ \hat{\lambda}_i &\rightarrow \sigma^2 b_2, & q + 1 \leq i \leq L.\end{aligned}\tag{7.34}$$

That is, when i is larger than q , the estimated eigenvalue $\hat{\lambda}_i$ converges to the right edge $\sigma^2 b_2$ of the support of F_{c,y,σ^2} . This means that any eigenvalues such that $\sigma^2 < \lambda_i \leq \sigma^2 \gamma(1 + \sqrt{c + y - cy})$ cannot be identified through the estimated eigenvalues and then show the optimality of this lower bound.

Modifying the result of [Wang and Yao \(2017\)](#), we can show that those extreme eigenvalues $\hat{\lambda}_i$ corresponding to $\lambda_i > \sigma^2 \gamma(1 + \sqrt{c + y - cy})$ satisfy Central Limiting Theorem and thus have the convergence rate of order $1/\sqrt{n}$. For the fluctuation of those eigenvalues which stick to the bulk, [Han et al. \(2016\)](#) showed that $n^{2/3}(\hat{\lambda}_{q+1} - \sigma^2 b_2)$ is asymptotically Tracy-Widom distributed. [Han et al. \(2018\)](#) established an asymptotic joint distribution for $(n^{2/3}(\hat{\lambda}_{q+1} - \sigma^2 b_2), n^{2/3}(\hat{\lambda}_{q+2} - \sigma^2 b_2), \dots, n^{2/3}(\hat{\lambda}_{q+k} - \sigma^2 b_2))$ for any fixed k . Thus, for any fixed $L > q$, $n^{2/3}(\hat{\lambda}_i - \sigma^2 b_2) = O_p(n^{-2/3})$ for $q + 1 \leq i \leq L$. The Spiked Fisher matrix \mathbf{F}_n satisfies Model Feature 2.1. The proof is finished. \square

Proof of Proposition 4.2. Let $\Sigma_y = cov(y_t, y_{t-1})$ be the lag-1 auto-covariance matrices of y_t and $\Sigma_x = cov(x_t, x_{t-1})$ the lag-1 auto-covariance matrix of x_t . As shown in [Li et al. \(2017\)](#), the sample auto-covariance matrix of y_t is

$$\hat{\Sigma}_y = \frac{1}{T} \sum_{t=2}^{T+1} y_t y_{t-1}' = \frac{1}{T} \sum_{t=2}^{T+1} (\mathbf{A}x_t + \varepsilon_t)(\mathbf{A}x_{t-1} + \varepsilon_{t-1})'$$

$$\begin{aligned}
&= \frac{1}{T} \sum_{t=2}^{T+1} \mathbf{A} x_t x'_{t-1} \mathbf{A}' + \frac{1}{T} \sum_{t=2}^{T+1} (\mathbf{A} x_t \varepsilon'_{t-1} + \varepsilon_t x'_{t-1} \mathbf{A}') + \frac{1}{T} \sum_{t=2}^{T+1} \varepsilon_t \varepsilon'_{t-1} \\
&:= \mathbf{P}_{\mathbf{A}} + \hat{\Sigma}_{\varepsilon},
\end{aligned} \tag{7.35}$$

where the matrix $\hat{\Sigma}_{\varepsilon} = \frac{1}{T} \sum_{t=2}^{T+1} \varepsilon_t \varepsilon'_{t-1}$ is the sample auto-covariance matrix of noise sequence $\{\varepsilon_t\}$. Notice that the matrix $\mathbf{P}_{\mathbf{A}}$ is of finite rank, then the matrix $\hat{\Sigma}_y$ can be viewed as a finite-rank perturbation of $\hat{\Sigma}_{\varepsilon}$. Since both $\hat{\Sigma}_{\varepsilon}$ and $\hat{\Sigma}_y$ are asymmetric matrices, [Li et al. \(2017\)](#) considered their singular values. This is equivalent to considering the square root of the eigenvalues of the matrices $\hat{\mathbf{M}}_{\varepsilon} := \hat{\Sigma}_{\varepsilon} \hat{\Sigma}'_{\varepsilon}$ and $\hat{\mathbf{M}}_y := \hat{\Sigma}_y \hat{\Sigma}'_y$, respectively.

Define $\hat{\Sigma}_y/\sigma^2 = \mathbf{P}_{\mathbf{A}}/\sigma^2 + \hat{\Sigma}_{\varepsilon}/\sigma^2$, we can reduce the problem to the case with $\sigma^2 = 1$. When $p/T \rightarrow y > 0$, [Li et al. \(2015\)](#) proved that the empirical spectral distribution of $\hat{\mathbf{M}}_{\varepsilon}$ almost surely converges to a non-random limiting distribution, whose Stieltjes transformation $\mathcal{S}(z)$ defined in (4.10) satisfies the equation

$$z^2 \mathcal{S}^3(z) - 2z(y-1) \mathcal{S}^2(z) + (y-1)^2 \mathcal{S}(z) - z \mathcal{S}(z) - 1 = 0.$$

This limiting spectral distribution is continuous with a compact support $[a_1 \mathbf{1}_{\{y \geq 1\}}, b_1]$, where

$$a_1 = (-1 + 20y + 8y^2 - (1 + 8y)^{3/2})/8,$$

$$b_1 = (-1 + 20y + 8y^2 + (1 + 8y)^{3/2})/8$$

From [Wang and Yao \(2016\)](#), the largest eigenvalue $\hat{\lambda}_{\varepsilon,1}$ of $\hat{\mathbf{M}}_{\varepsilon}$ almost surely converges to the right edge b_1 . Like the previous models, for any fixed $L > q_0 + 1$, and any $1 \leq i \leq L$ the largest eigenvalues $\hat{\lambda}_{\varepsilon,i}$ of $\hat{\mathbf{M}}_{\varepsilon}$ converge to the same value b_1 . Further, for general σ^2 , the result of [Li et al. \(2017\)](#) implies that the limiting spectral distribution of the perturbed matrix $\hat{\mathbf{M}}_y$ is identical to that of $\hat{\mathbf{M}}_{\varepsilon}$. They also built a phase transition phenomenon for those extreme eigenvalues $\hat{\lambda}_1 \geq \dots \geq \hat{\lambda}_q$. The following proposition confirms the optimality of the bound restriction $\mathcal{T}_1(i) < \mathcal{T}(b_1+)$ such that the corresponding q factors in $\mathbf{P}_{\mathbf{A}}$ can be identified.

Lemma 7.1 (Li et al. (2017)). Denote $\mathcal{T}(\cdot)$ as the T -transformation of the Limiting Spectral Distribution (LSD) for matrix $\hat{\mathbf{M}}_y/\sigma^4$. Suppose that the model (4.9) satisfies Assumptions 4.1 and 4.2, $\{\varepsilon_t\}$ are normally distributed and the loading matrix \mathbf{A} is standardized as $\mathbf{A}'\mathbf{A} = \mathbf{I}_k$. Let $\hat{\lambda}_i$, $1 \leq i \leq q_0$ denote the q_0 largest eigenvalues of $\hat{\mathbf{M}}_y$. Then for each $1 \leq i \leq q_0$, $\hat{\lambda}_i/\sigma^4$ converges almost surely to a limit β_i . Moreover,

$$\beta_i > b_1 \text{ when } \mathcal{T}_1(i) < \mathcal{T}(b_1+),$$

and

$$\beta_i = b_1 \text{ when } \mathcal{T}_1(i) \geq \mathcal{T}(b_1+)$$

where

$$\mathcal{T}_1(i) = \frac{2y\sigma^2\gamma_0(i) + \gamma_1(i)^2 - \sqrt{(2y\sigma^2\gamma_0(i) + \gamma_1(i)^2)^2 - 4y^2\sigma^4(\gamma_0(i)^2 - \gamma_1(i))^2}}{2\gamma_0(i)^2 - 2\gamma_1(i)^2}.$$

From this proposition, we can see that the bound for the number of common factors determined by the constraint $\mathcal{T}_1(i) < \mathcal{T}(b_1+)$ is optimal. That is, only q common factors in $\mathbf{P}_\mathbf{A}$ can be well separated from the noise ε_t 's theoretically. This is because $\hat{\lambda}_{q+1}$ will converge to b_1 and thus cannot be well separated from those large estimated eigenvalues of $\hat{\Sigma}_\varepsilon$ that tend to the right edge b_1 as well. \square

A justification of Proposition 4.2. By the results of Wang and Yao (2016), the condition (A1) holds. Further, under the assumption that the estimated eigenvalues $\hat{\lambda}_i$ for $i > q$ have the convergence rate of order $O_p(n^{-2/3})$, the condition (A2) in Model Feature 2.1 holds. Following the arguments used in Theorems 2.1 and 3.1, the results hold. \square

References

Bai, Z. and J. Yao (2008). Central limit theorems for eigenvalues in a spiked population model. In *Annales de l'Institut Henri Poincaré, Probabilités et Statistiques*, Volume 44, pp. 447–474. Institut Henri Poincaré.

- Baik, J. and J. W. Silverstein (2006). Eigenvalues of large sample covariance matrices of spiked population models. *Journal of Multivariate Analysis* 97(6), 1382–1408.
- Bao, Z., G. Pan, and W. Zhou (2015). Universality for the largest eigenvalue of sample covariance matrices with general population. *The Annals of Statistics* 43(1), 382–421.
- Benaych-Georges, F., A. Guionnet, and M. Maida (2011). Fluctuations of the extreme eigenvalues of finite rank deformations of random matrices. *Electronic Journal of Probability* 16(60), 1621–1662.
- Han, X., G. Pan, and Q. Yang (2018). A unified matrix model including both CCA and F matrices in multivariate analysis: the largest eigenvalue and its applications. *Bernoulli* 24(4B), 3447–3468.
- Han, X., G. Pan, and B. Zhang (2016). The tracy–widom law for the largest eigenvalue of F type matrices. *The Annals of Statistics* 44(4), 1564–1592.
- Li, Z., G. Pan, and J. Yao (2015). On singular value distribution of large-dimensional autocovariance matrices. *Journal of Multivariate Analysis* 137, 119–140.
- Li, Z., Q. Wang, and J. Yao (2017). Identifying the number of factors from singular values of a large sample auto-covariance matrix. *The Annals of Statistics* 45(1), 257–288.
- Passemier, D. and J. Yao (2012). On determining the number of spikes in a high-dimensional spiked population model. *Random Matrices: Theory and Applications* 1(01), 1150002.
- Passemier, D. and J. Yao (2014). Estimation of the number of spikes, possibly equal, in the high-dimensional case. *Journal of Multivariate Analysis* 127, 173–183.
- Wang, Q. and J. Yao (2016). Moment approach for singular values distribution of a large auto-covariance matrix. In *Annales de l’Institut Henri Poincaré, Probabilités et Statistiques*, Volume 52, pp. 1641–1666. Institut Henri Poincaré.

Wang, Q. and J. Yao (2017). Extreme eigenvalues of large-dimensional spiked fisher matrices with application. *The Annals of Statistics* 45(1), 415–460.